

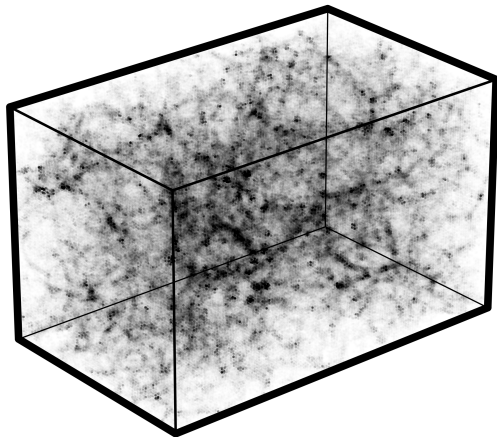
# Combining line intensity mapping & CMB lensing to probe the faint universe

Delon Shen

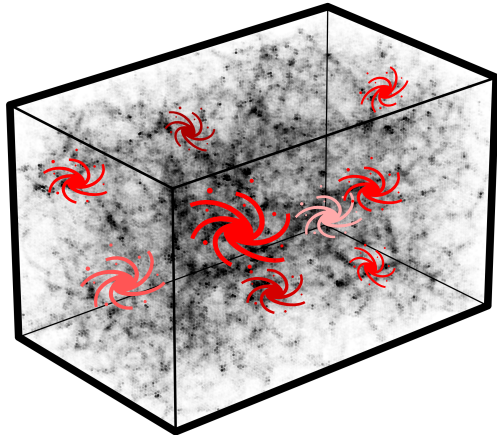
UChicago KICP Seminar — February 12, 2026

[arxiv:2507.17752](https://arxiv.org/abs/2507.17752) with Nickolas Kokron and Emmanuel Schaan  
published in Phys.Rev.D 113, 023521 (2026)

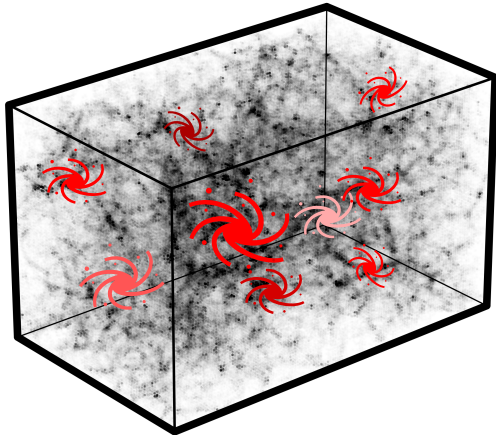
# Dark Matter



# Galaxies trace Dark Matter

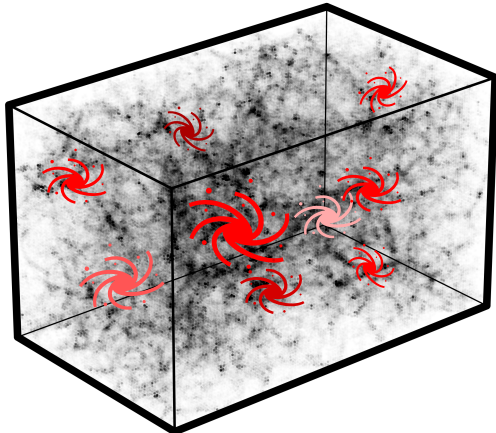


# Galaxies trace Dark Matter



~~Faint Galaxies~~  
(Hard to find but informative)

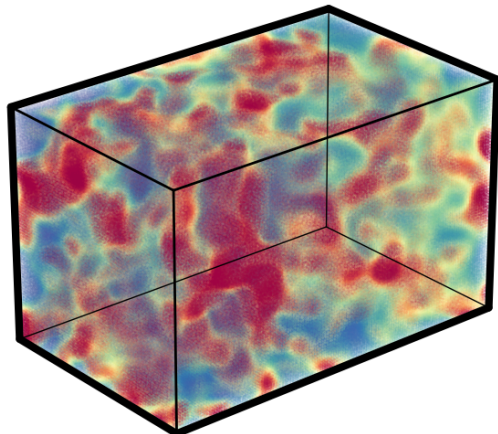
# Galaxies trace Dark Matter



~~Faint Galaxies~~  
(Hard to find but informative)

~~High-redshift~~  
(Not many galaxies have formed yet)

# Line Intensity Map traces Dark Matter

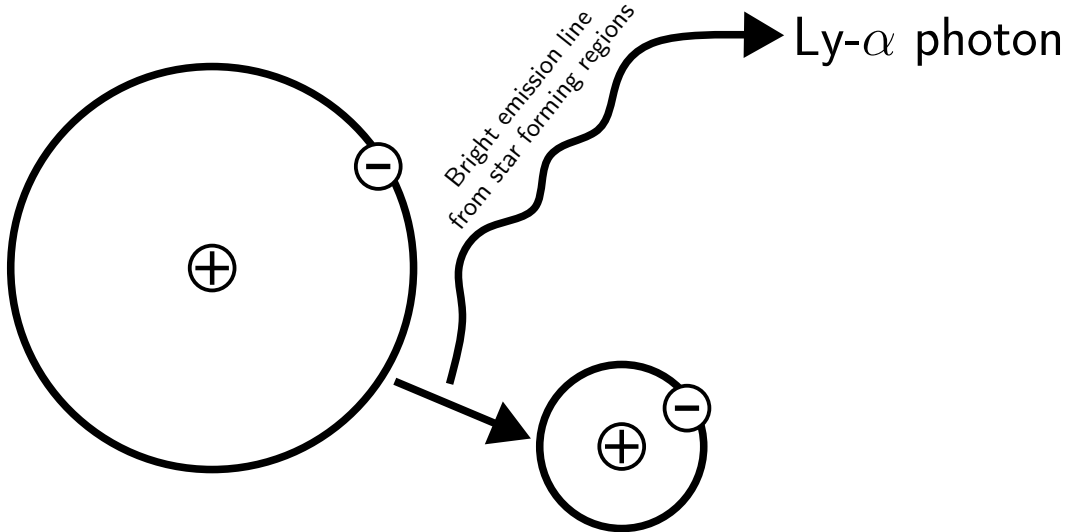


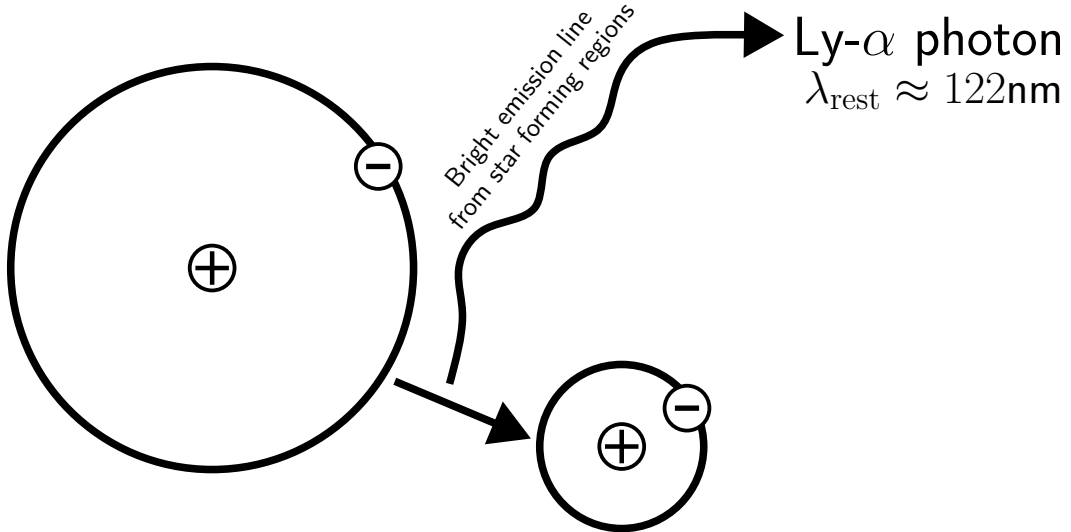
**Faint Galaxies**

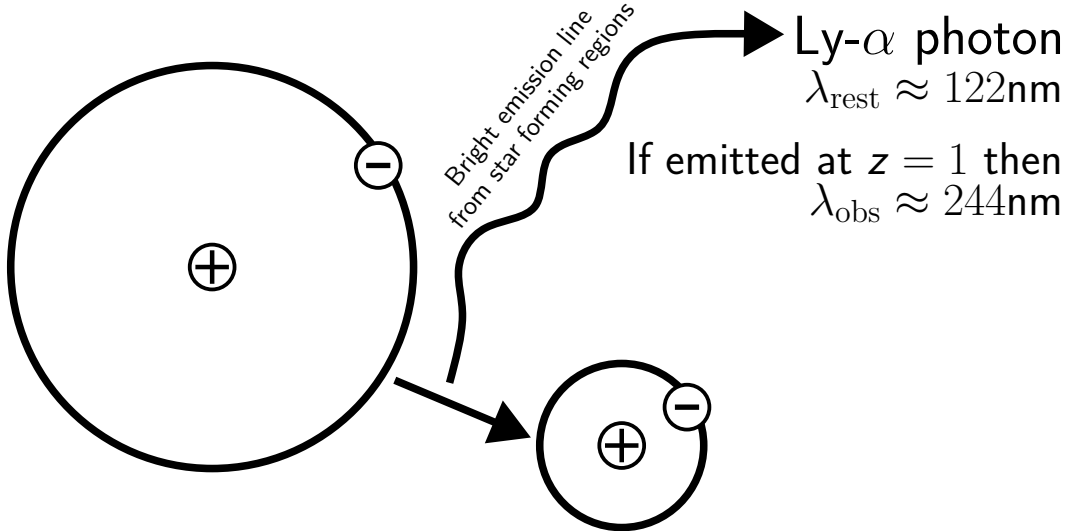
(Sums emission from many faint galaxies)

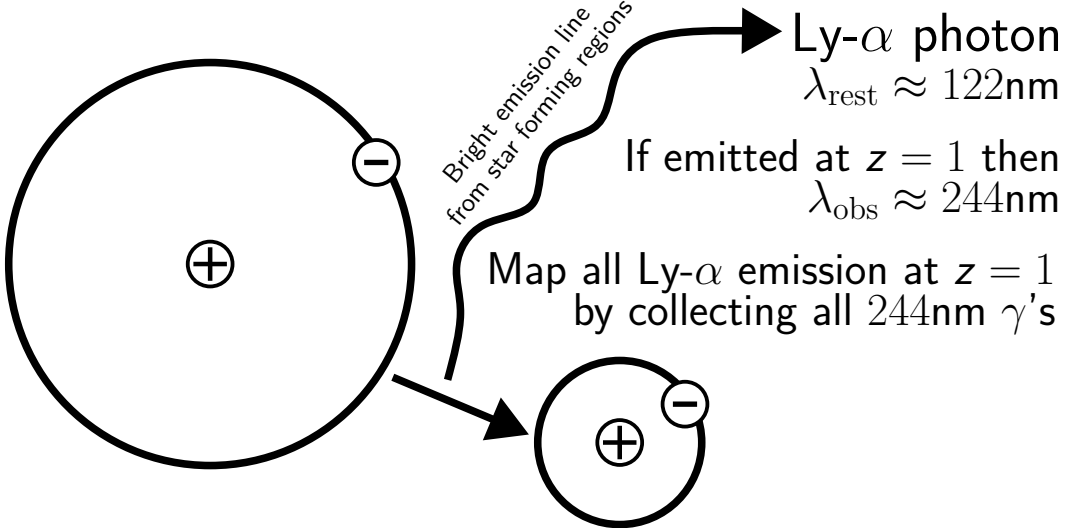
**High-redshift**

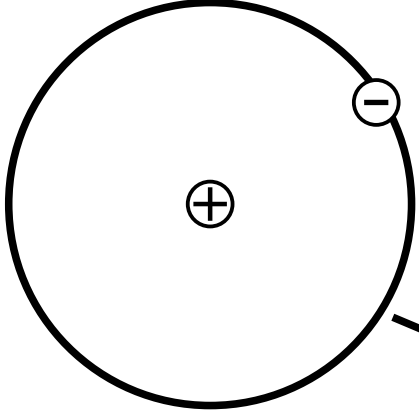
(Doesn't require galaxies to already have formed for a signal)











Bright emission line  
from star forming regions

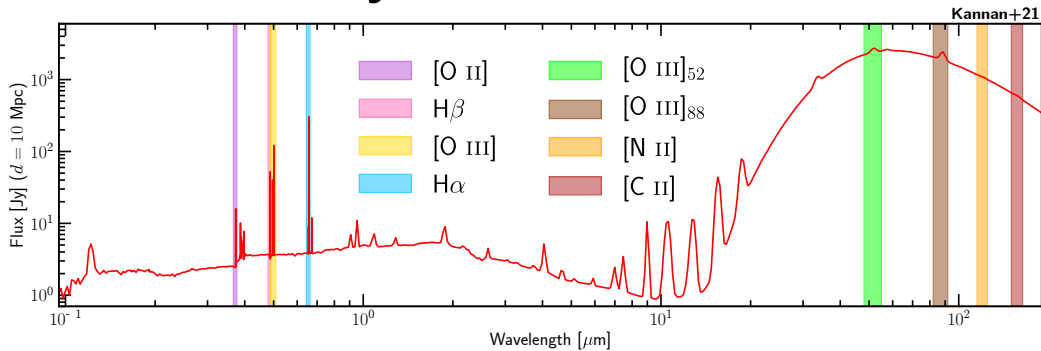
Ly- $\alpha$  photon  
 $\lambda_{\text{rest}} \approx 122\text{nm}$

If emitted at  $z = 1$  then  
 $\lambda_{\text{obs}} \approx 244\text{nm}$

Map all Ly- $\alpha$  emission at  $z = 1$   
by collecting all 244nm  $\gamma$ 's

Varying  $\lambda_{\text{obs}} \Rightarrow$  3-D map

# Many lines to observe

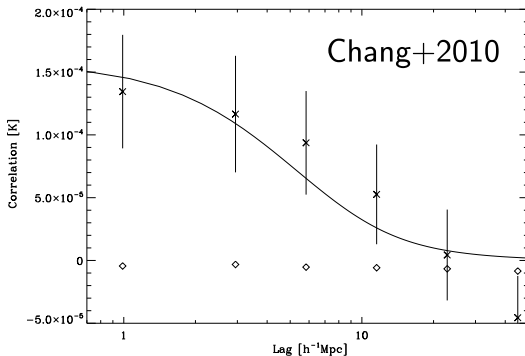


**Cross-correlations will be essential to  
realize the full science potential of LIM**

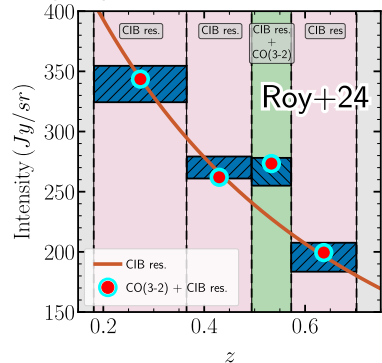
# Cross-correlations will be essential to realize the full science potential of LIM

Improve confidence and mitigate foreground/systematics  
(Most early detections have come from cross-correlations)

21cm from GBT x DEEP2



CO(3-2) from Planck x eBOSS



**Cross-correlations will be essential to  
realize the full science potential of LIM**

Enables new science directions. Some examples:

## **Cross-correlations will be essential to realize the full science potential of LIM**

Enables new science directions. Some examples:

Clustering-based redshift (help calibrate DES/LSST photo-z)

(Meenard+13, McQuinnWhite13, Rahman+13, Alonso+17, Cunningham+18...)

# Cross-correlations will be essential to realize the full science potential of LIM

Enables new science directions. Some examples:

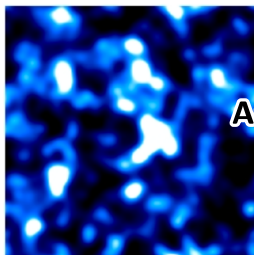
Clustering-based redshift (help calibrate DES/LSST photo-z)

(Meenard+13, McQuinnWhite13, Rahman+13, Alonso+17, Cunningham+18...)

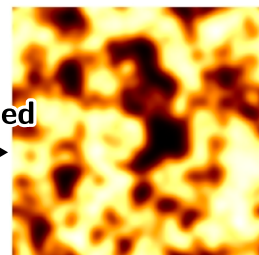
Multi-line intensity mapping

(Lidz+11, Kannan++, Sun++, Schaan+21, Cheng+24, Fronenberg+24, Libanore+25)

CO(2-1)  
during EOR



Anti-correlated  
↔



21cm  
during EOR

Lidz+11, Kovetz+17

## **Cross-correlations will be essential to realize the full science potential of LIM**

Enables new science directions. Some examples:

**Clustering-based redshift** (help calibrate DES/LSST photo-z)

(Meenard+13, McQuinnWhite13, Rahman+13, Alonso+17, Cunningham+18...)

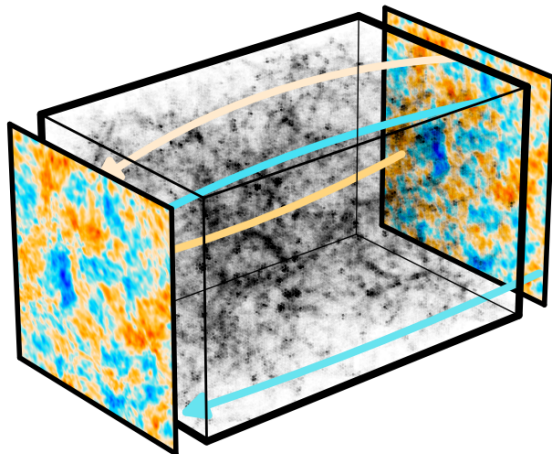
**Multi-line intensity mapping**

(Lidz+11, Kannan++, Sun++, Schaan+21, Cheng+24, Fronenberg+24, Libanore+25)

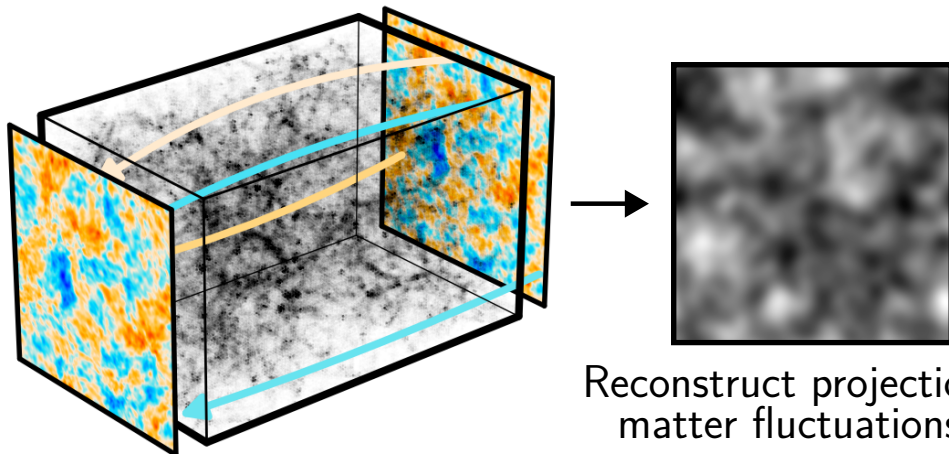
Correlate with weak lensing to  
directly probe the line emssion-matter connection

**This talk**

# CMB photons lensed by Dark Matter

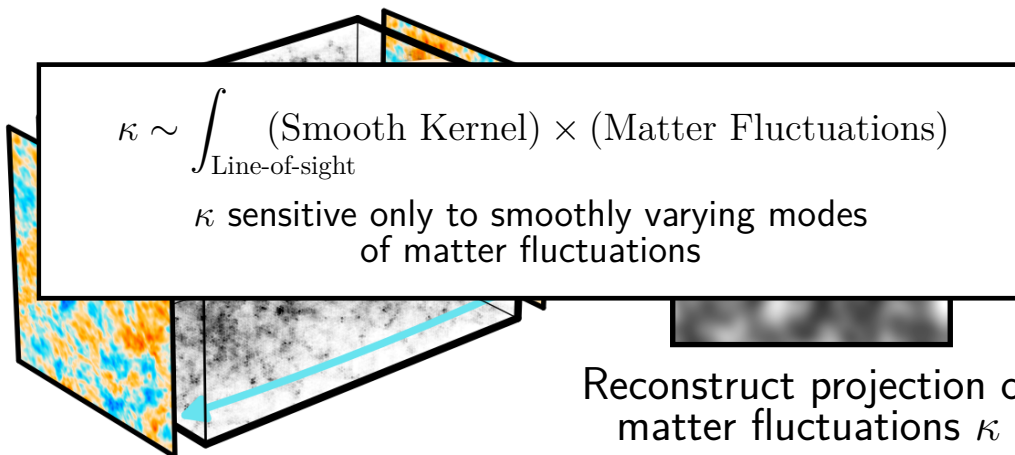


# CMB photons lensed by Dark Matter



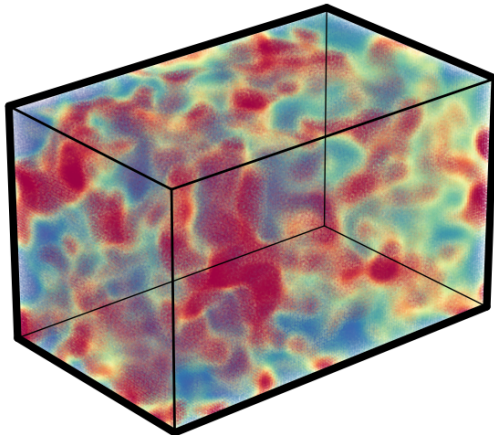
Reconstruct projection of  
matter fluctuations  $\kappa$

# CMB photons lensed by Dark Matter

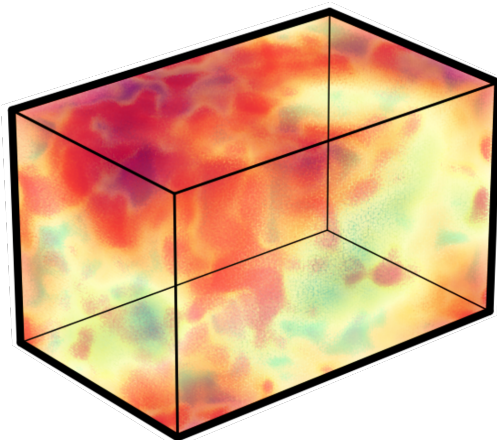


Reconstruct projection of  
matter fluctuations  $\kappa$

# Line Intensity Map traces Dark Matter

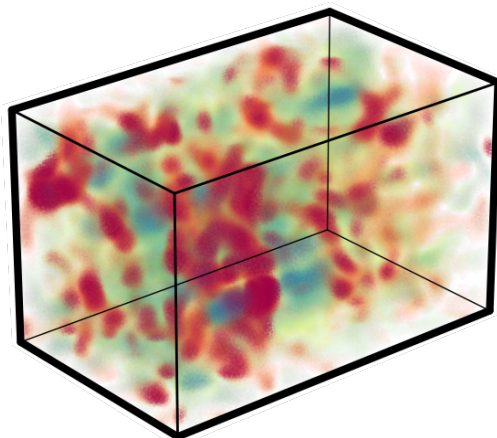


# Line Intensity Map traces Dark Matter



**Contaminated by  
Galactic foregrounds**  
Spectrally smooth and bright

# **Line Intensity Map** traces Dark Matter



**Contaminated by  
Galactic foregrounds**

Spectrally smooth and bright



**(High-pass) filter out  
smoothly varying modes**

Removes Galactic foregrounds (and  
some cosmological line emission)

**LIM** ..... removes smoothly varying modes

**LIM** ..... removes smoothly varying modes  
**CMB lensing** ... only smoothly varying modes

**LIM** ..... removes smoothly varying modes  
**CMB lensing** ... only smoothly varying modes

Symmetries of the universe make this  
lack of overlap look problematic

# Symmetries of background universe

Isotropic and Homogeneous

$$\rho_m(\mathbf{x}) = \bar{\rho}_m$$

# Symmetries of background universe

Isotropic and Homogeneous

$$\rho_m(\mathbf{x}) = \bar{\rho}_m \Rightarrow \tilde{\rho}_m(\mathbf{k}) \sim \text{Dirac Delta}(\mathbf{k})$$

# Symmetries of background universe

Isotropic and Homogeneous

$$\rho_m(\mathbf{x}) = \bar{\rho}_m \Rightarrow \tilde{\rho}_m(\mathbf{k}) \sim \text{Dirac Delta}(\mathbf{k})$$

$$\tilde{\rho}_m(\mathbf{k})\tilde{\rho}_m(\mathbf{k}') = 0 \text{ unless } \mathbf{k} = \mathbf{k}'$$

# Symmetries of fluctuating universe

Statistically Isotropic and Homogeneous

$$\rho_m(\mathbf{x}) = \bar{\rho}_m(1 + \delta_m(\mathbf{x})) \text{ (statistical field)}$$

# Symmetries of fluctuating universe

Statistically Isotropic and Homogeneous

$$\rho_m(\mathbf{x}) = \bar{\rho}_m(1 + \delta_m(\mathbf{x})) \text{ (statistical field)}$$

$$\langle \delta_m(\mathbf{k}) \delta_m(\mathbf{k}') \rangle = 0 \text{ unless } \mathbf{k} = \mathbf{k}'$$

Short-wavelength  
and Long-wavelength  
matter fluctuations  
are uncorrelated

# **Line Intesity Mapping**

Loses *long-wavelength* fluctuations  
because of Galactic foregrounds

## **Line Intesity Mapping**

Loses *long-wavelength* fluctuations  
because of Galactic foregrounds

## **CMB lensing**

Loses *short-wavelength* fluctuations  
because of the projection kernel

# Line Intensity Map

Loses long

Claim by previous works:  
Direct correlation of  
LIM with CMB lensing  
is hopeless

fluctuations  
of the projection kernel

A.Obuljen, E.Castorina, F.Villaescusa-Navarro, M.Viel 2017

D.Li, H.M.Zhu, U.L.Pen 2019

C.Modi, M.White, A.Slosar, E.Castorina 2019

K.Moodley, W.Naidoo, H.Prince, A.Penin 2023

e.g.

# Line Intensity Map

Loses long

Claim by previous works:

Direct correlation of  
LIM with Any projected field  
is hopeless

fluctuations  
of the projection kernel

A.Obuljen, E.Castorina, F.Villaescusa-Navarro, M.Viel 2017

D.Li, H.M.Zhu, U.L.Pen 2019

C.Modi, M.White, A.Slosar, E.Castorina 2019

K.Moodley, W.Naidoo, H.Prince, A.Penin 2023

e.g.

# Line Intensity Map

Loses long

Claim by ~~me~~ ~~other authors~~:

Direct correlation of  
LIM with Any projected field  
is ~~hopeless~~ fine

fluctuations  
of the projection kernel

A.Obuljen, E.Castorina, F.Villaescusa-Navarro, M.Viel 2017

D.Li, H.M.Zhu, U.L.Pen 2019

C.Modi, M.White, A.Slosar, E.Castorina 2019

K.Moodley, W.Naidoo, H.Prince, A.Penin 2023

e.g.

Short and long wavelength **matter fluctuations** are uncorrelated

Short and long wavelength **matter fluctuations** are uncorrelated

Remove long-wavelength fluctuations from LIM



Remove long-wavelength matter fluctuations?

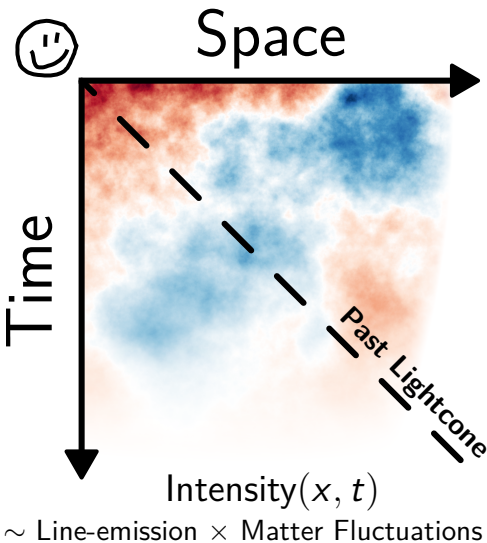
Short and long wavelength **matter fluctuations** are uncorrelated

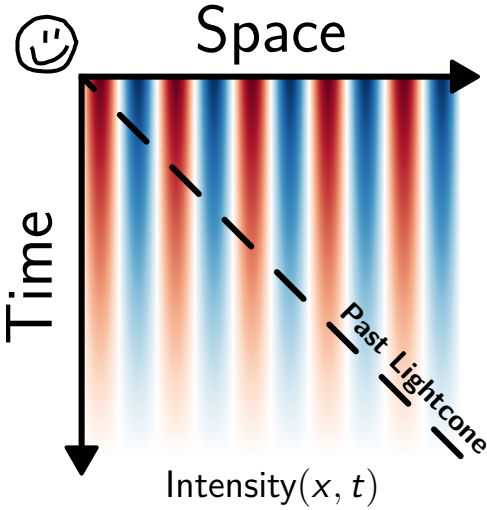
Remove long-wavelength fluctuations from LIM



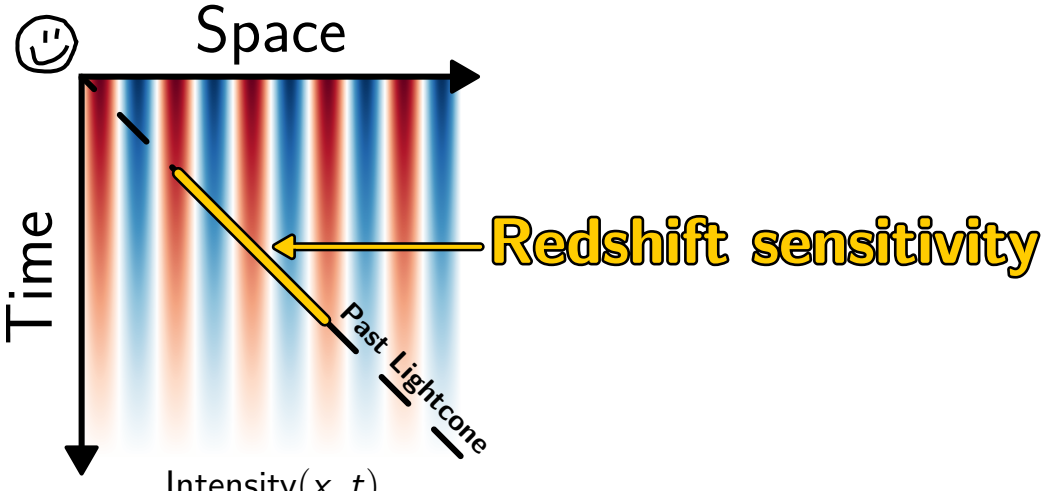
Remove long-wavelength matter fluctuations?

**No**, observations restricted to past lightcone

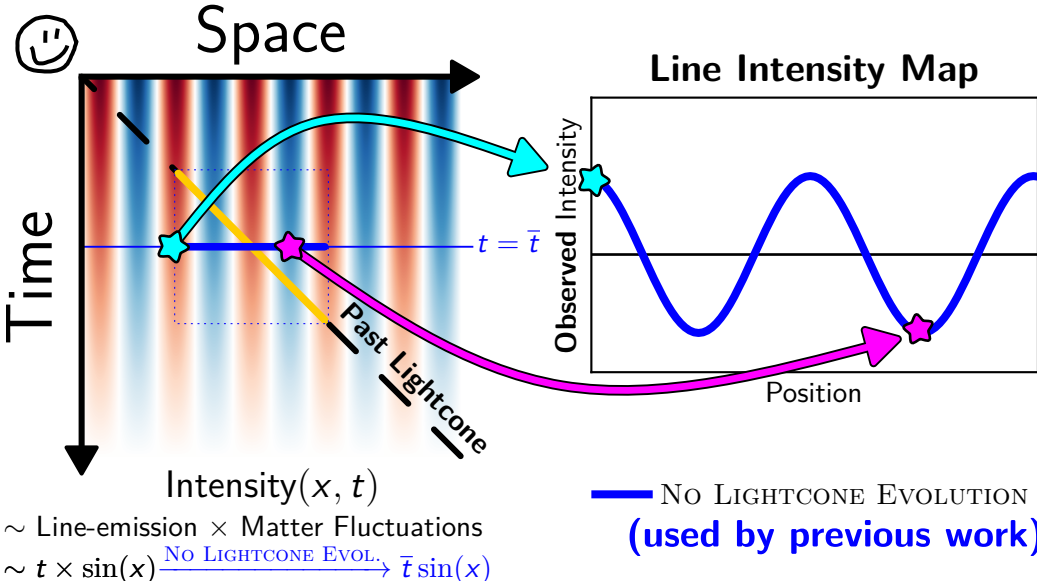


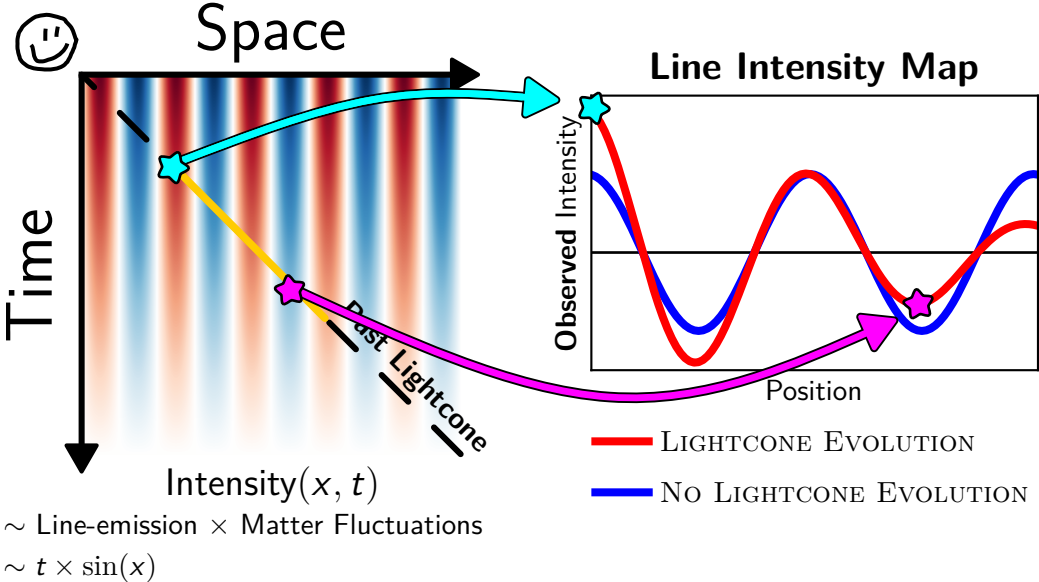


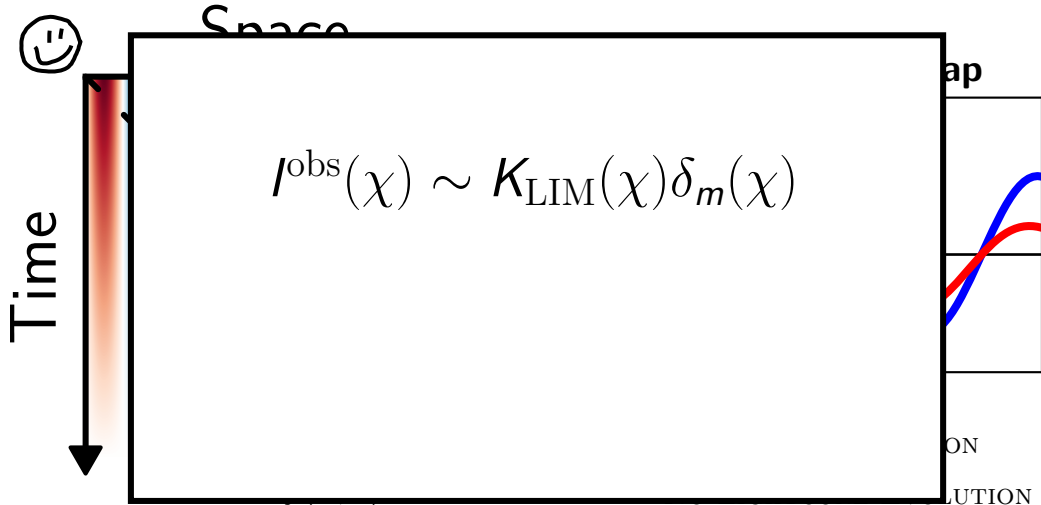
$\sim$  Line-emission  $\times$  Matter Fluctuations  
 $\sim t \times \sin(x)$



$\sim$  Line-emission  $\times$  Matter Fluctuations  
 $\sim t \times \sin(x)$

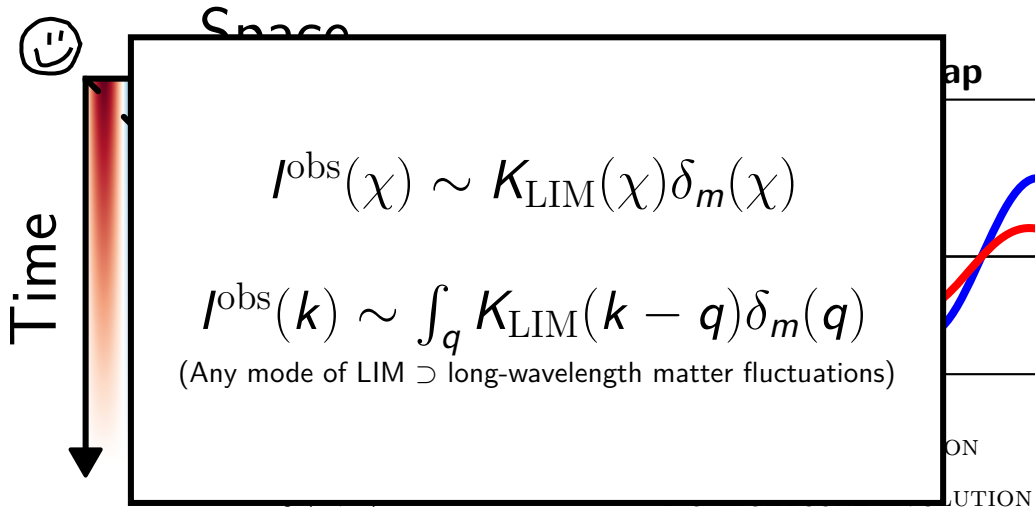






$\sim$  Line-emission  $\times$  Matter Fluctuations

$\sim t \times \sin(x)$



$\sim$  Line-emission  $\times$  Matter Fluctuations

$\sim t \times \sin(x)$



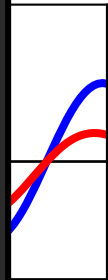
Time



Space

ap

Long-wavelength modes  
lost to bright foregrounds  
**may not be problematic!**  
(Any mode of LIM  $\supset$  long-wavelength matter fluctuations)



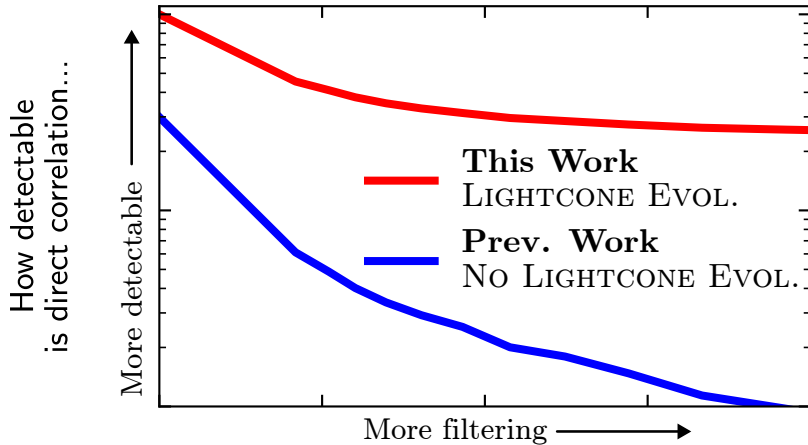
ON

LUTION

$\sim$  Line-emission  $\times$  Matter Fluctuations

$\sim t \times \sin(x)$

# Detectability in Toy Model



...as you filter out more long-wavelength modes?

**Why is lightcone evolution  
important in LIM but not galaxy  
surveys?**

$$I(z) \sim \int_M n(\chi(z), z; M) \times L(z, M)$$

$I(z) \sim \int_M$  [Number density of halos at position  
 $\chi(z)$  at redshift  $z$  with mass  $M$ ]  
 $\times$  [Luminosity of line emission by a halo  
at redshift  $z$  with mass  $M$ ]

## **Minimal model for halos**

(linear bias  $\times$  linear matter field)

$$n = \bar{n} + \delta n$$

$$\delta n = \bar{n}(b \times D\delta_m^0)$$

## Minimal model for halos

(linear bias  $\times$  linear matter field)

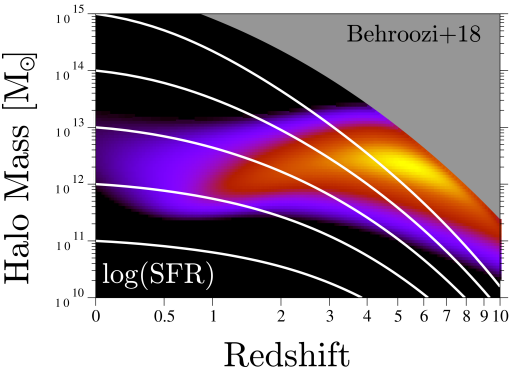
$$n = \bar{n} + \delta n$$

$$\delta n = \bar{n}(b \times D\delta_m^0)$$

## Minimal model for luminosity-halo relation

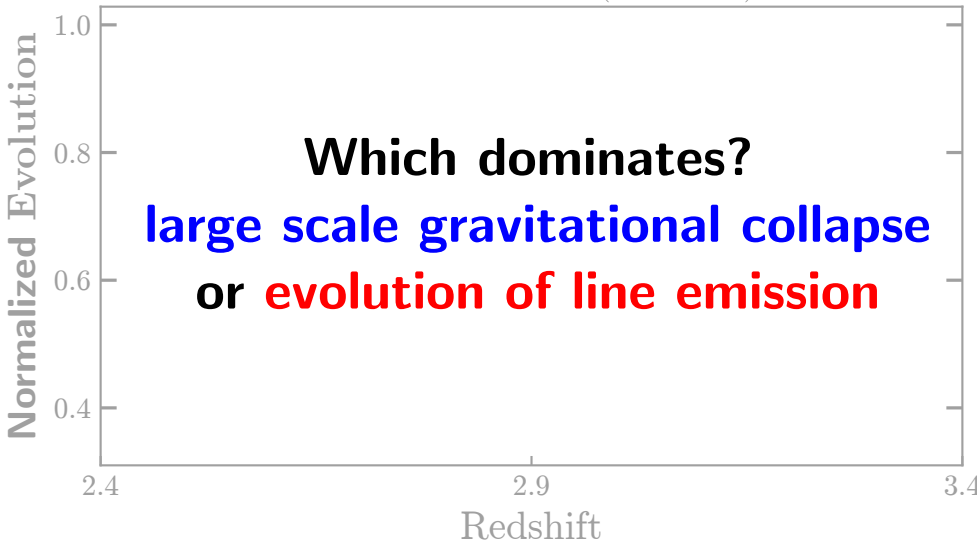
(luminosity  $\sim$  SFR)

UniverseMachine Average SFR

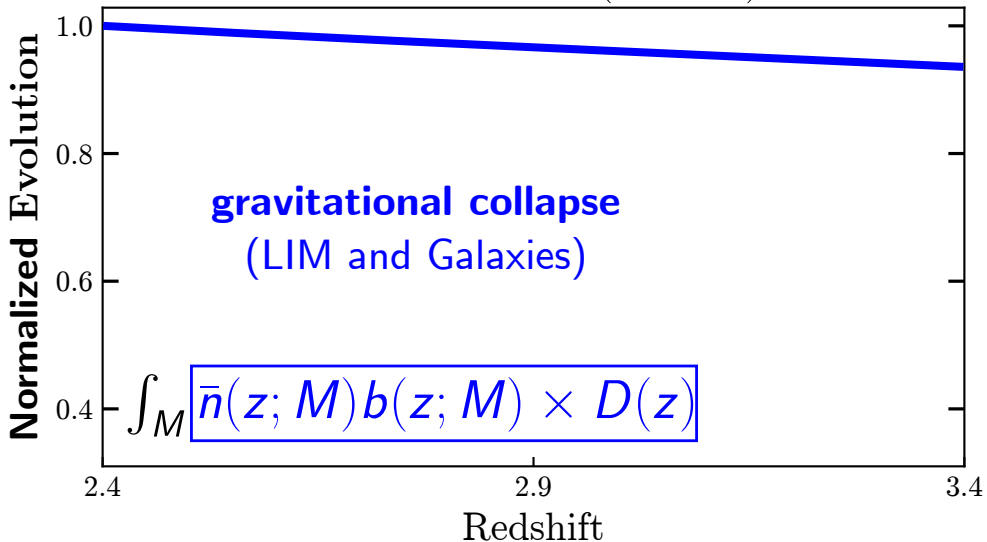


$$\delta I(z) \sim \int_M \underbrace{\bar{n}(z; M) b(z; M) \times D(z)}_{\text{Large-scale gravitational collapse sources evolution for both galaxy surveys and LIM...}} \underbrace{L(M, z)}_{\text{...but LIM has an additional astrophysical source of evolution}}$$

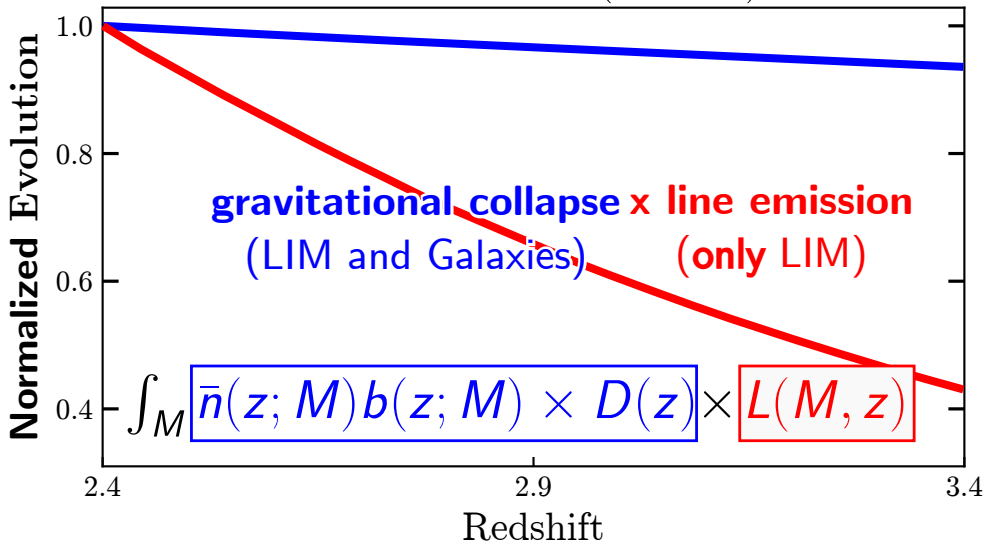
# COMAP CO( $1 \rightarrow 0$ )



# COMAP CO( $1 \rightarrow 0$ )



# COMAP CO( $1 \rightarrow 0$ )



1.0

# The twist

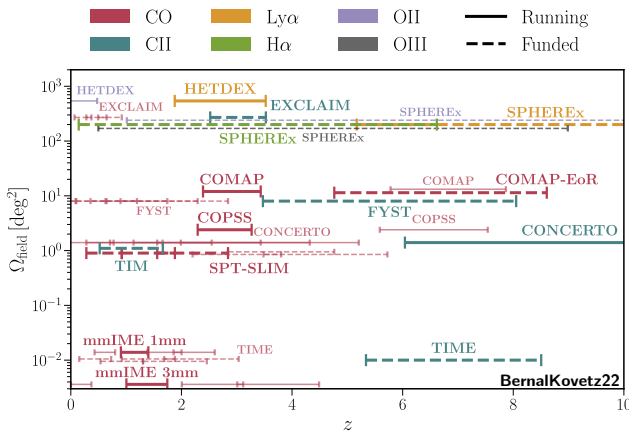
$T_{\text{astrophysics}} \ll T_{\text{gravity}}$

2.5

3.4

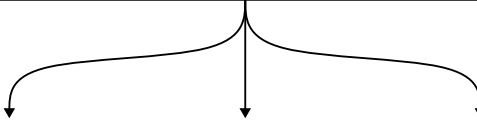
Redshift

Experiment	CHIME	HETDEX	COMAP	CCAT	SPHEREx
Line	HI(21cm)	Ly- $\alpha$	CO(1→0)	[CII]	Ly- $\alpha$
$\nu_{\text{obs}}$	617-710 MHz	545-857 THz	26-34 GHz	210-420 GHz	270-400 THz
$z_{\text{obs}}$	1.0 - 1.3	1.9 - 3.5	2.4 - 3.4	3.5 - 8.1	5.2 - 8



$$\mathbf{SNR}^2 \sim \langle \text{LIM}_\ell(\chi) \kappa_{-\ell} \rangle \cdot [\text{Cov}(\chi, \chi')]^{-1} \cdot \langle \text{LIM}_\ell(\chi') \kappa_{-\ell} \rangle$$

$$\langle \phi_{\ell}(\bullet) \psi_{\mathbf{L}}(\bullet) \rangle' \approx \int_{\bar{\chi}} 2\bar{\chi} \int_{-1}^1 d\delta \frac{K_{\phi}(\bar{\chi}(1-\delta); \bullet) K_{\psi}(\bar{\chi}(1+\delta); \bullet)}{\bar{\chi}^2} \int_{k'_{\parallel}} e^{ik'_{\parallel} \times 2\bar{\chi}\delta} P^{\Phi\Psi} \left( k^2 = {k'_{\parallel}}^2 + \frac{\ell(\ell+1)}{\bar{\chi}^2(1-\delta^2)} \right)$$


 $\mathbf{SNR}^2 \sim \langle \text{LIM}_{\ell}(\chi) \kappa_{-\ell} \rangle \cdot [\text{Cov}(\chi, \chi')]^{-1} \cdot \langle \text{LIM}_{\ell}(\chi') \kappa_{-\ell} \rangle$

$$\langle \phi_\ell(\bullet) \psi_L(\bullet) \rangle' \approx \int_{\bar{\chi}} 2\bar{\chi} \int_{-1}^1 d\delta \frac{K_\phi(\bar{\chi}(1-\delta); \bullet) K_\psi(\bar{\chi}(1+\delta); \bullet)}{\bar{\chi}^2} \int e^{ik'_\parallel \times 2\bar{\chi}\delta} P^{\Phi\Psi} \left( k^2 = k'_\parallel^2 + \frac{\ell(\ell+1)}{\bar{\chi}^2(1-\delta^2)} \right)$$

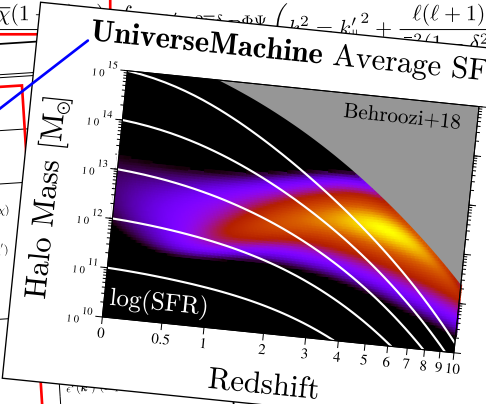
2-D Projected Field $\phi_\ell(\bullet)$ (Sec. IV A)	Projection Kernel $K_\phi(\chi'; \bullet)$	3-D Unprojected Field $\Phi(k')$
CMB Lensing $\kappa_\ell$ (Sec. III A)	$K_\kappa(\chi') = \frac{3H_0^2\Omega_{m,0}}{2a(\chi')} \frac{\chi'(\chi_* - \chi')}{\chi_*} \times D(\chi')$	Linear Matter Field $\delta_m^0(k')$
Line Intensity Map $I_\ell(\chi)$ (Sec. III B 1)	$K_{\text{LIM}}(\chi'; \chi) = \frac{\langle \rho_L \rangle(\chi') b_L(\chi')}{4\pi\nu_{\text{line}} H(\chi')} \times D(\chi') \Pi(\chi') \delta^{(D)}(\chi' - \chi)$	Linear Matter Field $\delta_m^0(k')$
Low-Pass Filtered LIM $I_\ell^{\text{LoA}}(\chi)$ (Sec. III B 3)	$K_{\text{LIM}}^{\text{LoA}}(\chi'; \chi) = \frac{\langle \rho_L \rangle(\chi') b_L(\chi')}{4\pi\nu_{\text{rest}} H(\chi')} \times D(\chi') \Pi(\chi') \text{LoA}(\chi - \chi')$	Linear Matter Field $\delta_m^0(k')$
High-Pass Filtered LIM $I_\ell^{\text{HiA}}(\chi)$ (Sec. III B 3)	$K_{\text{LIM}}^{\text{HiA}}(\chi'; \chi) = K_{\text{LIM}}(\chi'; \chi) - K_{\text{LIM}}^{\text{LoA}}(\chi'; \chi)$	Linear Matter Field $\delta_m^0(k')$
Instrumental LIM Noise $\epsilon_\ell^I(\chi)$ (Sec. III B 2)	$K_{\epsilon, \text{LIM}}(\chi'; \chi) = \Pi(\chi') \delta^{(D)}(\chi' - \chi)$	Gaussian White Noise $\epsilon^I(k')$ (Eq. (22))
Low Pass Filtered LIM Noise $\epsilon_\ell^{\text{I,LoA}}(\chi)$ (Sec. III B 3)	$K_{\epsilon, \text{LIM}}^{\text{LoA}}(\chi'; \chi) = \Pi(\chi') \text{LoA}(\chi - \chi')$	Gaussian White Noise $\epsilon^I(k')$ (Eq. (22))
High-Pass Filtered LIM Noise $\epsilon_\ell^{\text{I,HiA}}(\chi)$ (Sec. III B 3)	$K_{\epsilon, \text{LIM}}^{\text{HiA}}(\chi'; \chi) = K_{\epsilon, \text{LIM}}(\chi'; \chi) - K_{\epsilon, \text{LIM}}^{\text{LoA}}(\chi'; \chi)$	Gaussian White Noise $\epsilon^I(k')$ (Eq. (22))

$\langle \text{LIM}_\ell(\chi') \kappa_{-\ell} \rangle$

$$\langle \phi_\ell(\bullet) \psi_L(\bullet) \rangle' \approx \int_{\bar{\chi}} 2\bar{\chi} \int_{-1}^1 d\delta \frac{K_\phi(\bar{\chi}(1-\delta); \bullet) K_\psi(\bar{\chi}(1-\delta); \bullet)}{\bar{\chi}^2}$$

UniverseMachine Average SFR

2-D Projected Field $\phi_\ell(\bullet)$ (Sec. IV A)	Projection Kernel $K_\phi(x'; \bullet)$
CMB Lensing $\kappa_\ell$ (Sec. III A)	$K_\kappa(x') = \frac{3H_0^2 \Omega_{m,0}}{2a(x')} \frac{x'(x_* - x')}{x_*} \times D(x')$
Line Intensity Map $I_\ell(x)$ (Sec. III B 1)	$K_{\text{LIM}}(x'; x) = \frac{\langle \rho_L \rangle(x') b_L(x')}{4\pi\nu_{\text{line}} H(x')} \times D(x') \Pi(x') \delta^{(D)}(x' - x)$
Low-Pass Filtered LIM $I_\ell^{\text{LoA}}(x)$ (Sec. III B 3)	$K_{\text{LIM}}^{\text{LoA}}(x'; x) = \frac{\langle \rho_L \rangle(x') b_L(x')}{4\pi\nu_{\text{rest}} H(x')} \times D(x') \Pi(x') \text{LoA}(x - x')$
High-Pass Filtered LIM $I_\ell^{\text{HiA}}(x)$ (Sec. III B 3)	$K_{\text{LIM}}^{\text{HiA}}(x'; x) = K_{\text{LIM}}(x'; x) - K_{\text{LIM}}^{\text{LoA}}(x'; x)$
Instrumental LIM Noise $\epsilon_\ell^I(x)$ (Sec. III B 2)	$K_{\epsilon,\text{LIM}}(x'; x) = \Pi(x') \delta^{(D)}(x' - x)$
Low Pass Filtered LIM Noise $\epsilon_\ell^{\text{LoA}}(x)$ (Sec. III B 3)	$K_{\epsilon,\text{LIM}}^{\text{LoA}}(x'; x) = \Pi(x') \text{LoA}(x - x')$
High-Pass Filtered LIM Noise $\epsilon_\ell^{\text{HiA}}(x)$ (Sec. III B 3)	$K_{\epsilon,\text{LIM}}^{\text{HiA}}(x'; x) = K_{\epsilon,\text{LIM}}(x'; x) - K_{\epsilon,\text{LIM}}^{\text{LoA}}(x'; x)$



$$\langle \phi_\ell(\bullet) \psi_L(\bullet) \rangle' \approx \int_{\bar{\chi}} 2\bar{\chi} \int_{-1}^1 d\delta \frac{K_\phi(\bar{\chi}(1-\delta); \bullet) K_\psi(\bar{\chi}(1-\delta); \bullet)}{\bar{\chi}^2}$$

UniverseMachine Average SFR  
 $\left( \omega_{1,2} = k_u'^2 + \frac{\ell(\ell+1)}{-2\gamma_1 - \delta^2} \right)$

2-D Projected Field  
 $\phi_\ell(\bullet)$  (Sec. IV A)

CM  
 $\kappa_\ell$  (Sec. III A)

Line Intensity Map  
 $I_\ell(\chi)$  (Sec. III B 1)

Low-Pass Filtered LIM  
 $I_\ell^{LoA}(\chi)$  (Sec. III B 3)

High-Pass Filtered LIM  
 $I_\ell^{HiA}(\chi)$  (Sec. III B 3)

Instrumental LIM Noise  
 $\epsilon_\ell^I(\chi)$  (Sec. III B 2)

Low Pass Filtered LIM Noise  
 $\epsilon_\ell^{I,LoA}(\chi)$  (Sec. III B 3)

High-Pass Filtered LIM Noise  
 $\epsilon_\ell^{I,HiA}(\chi)$  (Sec. III B 3)

Projection Kernel  
 $K_\phi(\chi'; \bullet)$

$$= \frac{v_\ell^2 \Omega}{4\pi} \chi' \times D(\chi')$$

$$K_{LIM}(\chi'; \chi) = \frac{\langle \rho_L \rangle(\chi') b_L(\chi')}{4\pi \nu_{line} H(\chi')} \times D(\chi') \Pi(\chi')$$

$$K_{e,LIM}^{LoA}(\chi'; \chi) = \frac{\langle \rho_L \rangle(\chi') b_L(\chi')}{4\pi \nu_{rest} H(\chi')} \times D(\chi') \Pi(\chi') Lo_A(\chi - \chi')$$

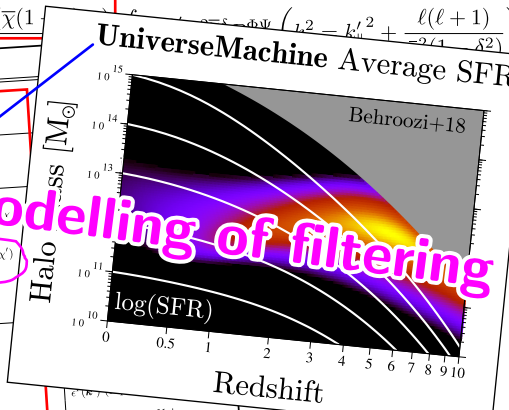
$$K_{e,LIM}^{HiA}(\chi'; \chi) = K_{e,LIM}(\chi'; \chi) - K_{e,LIM}^{LoA}(\chi'; \chi)$$

$$K_{e,LIM}(\chi'; \chi) = \Pi(\chi') \delta^{(D)}(\chi' - \chi)$$

$$K_{e,LIM}^{LoA}(\chi'; \chi) = \Pi(\chi') Lo_A(\chi - \chi')$$

$$K_{e,LIM}^{HiA}(\chi'; \chi) = K_{e,LIM}(\chi'; \chi) - K_{e,LIM}^{LoA}(\chi'; \chi)$$

**Analytical modelling of filtering**



$e^I(k')$   
 Gaussian White Noise  
 $e^I(k')$  (Eq. (22))

$$\langle \phi_\ell(\bullet) \psi_L(\bullet) \rangle' \approx \int \frac{2\chi}{\chi} J$$

2-D Projected Field  
 $\phi_\ell(\bullet)$  (Sec. IV A)

CM  
 $\kappa_\ell$  (Sec. III A)

Line Intensity Map  
 $I_\ell(\chi)$  (Sec. III B 1)

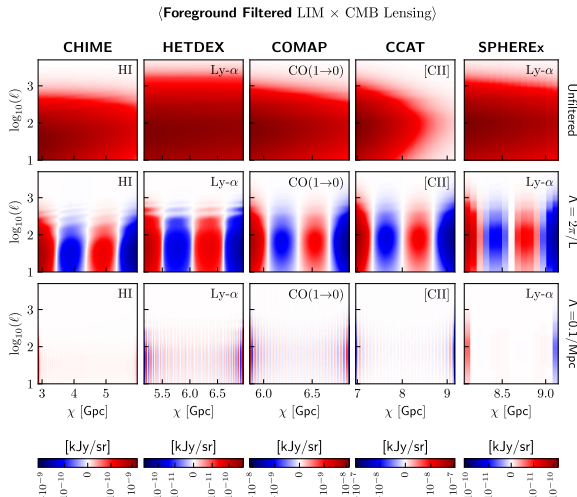
Low-Pass Filtered LIM  
 $I_\ell^{\text{LoP}}(\chi)$  (Sec. III B 3)

High-Pass Filtered LIM  
 $I_\ell^{\text{HiP}}(\chi)$  (Sec. III B 3)

Instrumental LIM Noise  
 $\epsilon_\ell^I(\chi)$  (Sec. III B 2)

Low Pass Filtered LIM Noise  
 $\epsilon_\ell^{I,\text{LoP}}(\chi)$  (Sec. III B 3)

High-Pass Filtered LIM Noise  
 $\epsilon_\ell^{I,\text{HiP}}(\chi)$  (Sec. III B 3)

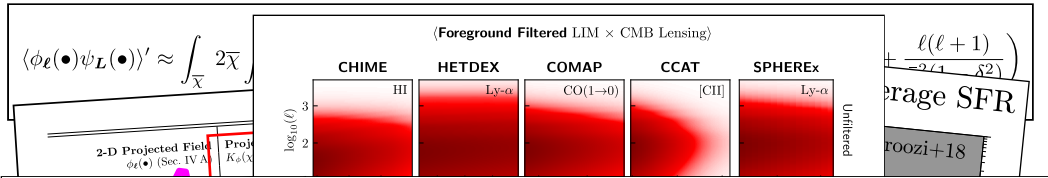


$$+ \frac{\ell(\ell+1)}{-2\ell_1 - \delta_2} \Big)$$

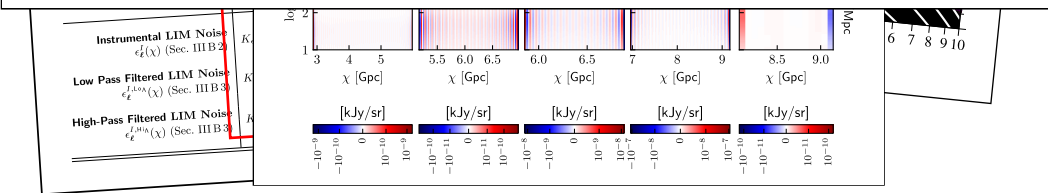
verage SFR

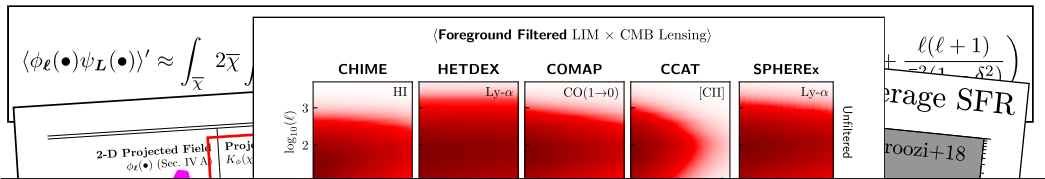
roozi+18

pring

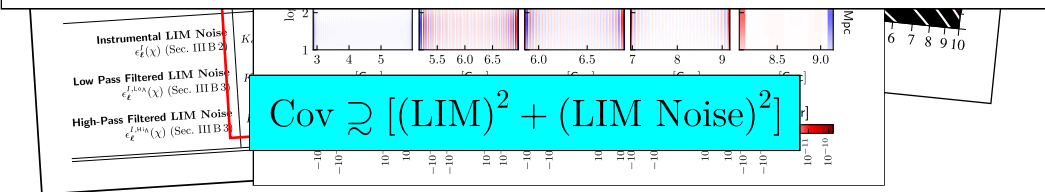


$$\text{SNR}^2 \sim \langle \text{LIM}_\ell(\chi) \kappa_{-\ell} \rangle \cdot [\text{Cov}(\chi, \chi')]^{-1} \cdot \langle \text{LIM}_\ell(\chi') \kappa_{-\ell} \rangle$$





$$\text{SNR}^2 \sim \langle \text{LIM}_\ell(\chi) \kappa_{-\ell} \rangle \cdot [\text{Cov}(\chi, \chi')]^{-1} \cdot \langle \text{LIM}_\ell(\chi') \kappa_{-\ell} \rangle$$



$$\langle \phi_\ell(\bullet) \rangle$$

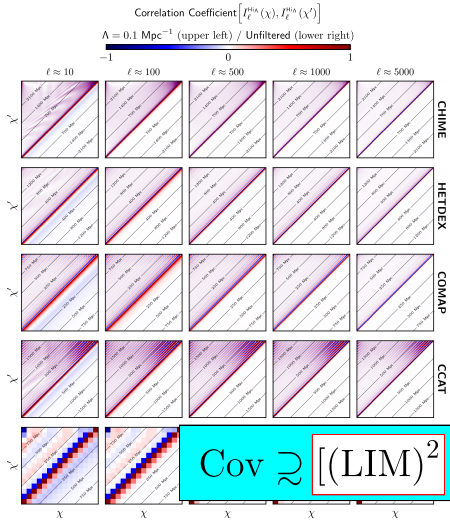
$$\frac{P_{\text{CHIME}}^{\epsilon_I}}{0.83 \text{ Mpc}^3 (\text{kJy/sr})^2} \approx \left( \frac{\Omega_{\text{field}}}{31000 \text{ deg}^2} \right) \left( \frac{\tau_{\text{survey}}}{1 \text{ yr}} \right)^{-1} \left( \frac{T_{\text{system}}}{55 \text{ K}} \right)^2 \left( \frac{N_{\text{ant}}}{256} \right)^{-2} \left( \frac{N_{\text{pol}}}{2} \right)^{-1} \left( \frac{N_{\text{cyl}}}{4} \right)^{-2} \left( \frac{\nu_{\text{obs}}}{663 \text{ MHz}} \right) \left( \frac{\Gamma(\nu_{\text{obs}})}{32.1 \text{ Gpc}^3} \right) \left( \frac{\Delta b^2}{10^4 \text{ m}^2} \right)^2 \left( \frac{d_{\text{ant}}}{0.3048 \text{ m}} \right)^{-3} \left( \frac{w_{\text{cyl}}}{20 \text{ m}} \right)^{-2} \left( \frac{\eta}{0.7} \right)^{-3}$$

$$\frac{P_{\text{HETDEX}}^{\epsilon_I}}{1.14 \text{ Mpc}^3 (\text{kJy/sr})^2} \approx \left( \frac{P_{\delta V}^{\epsilon_F}}{10^{-34} \text{ erg}^2 \text{ s}^{-2} \text{ cm}^{-4}} \right) \left( \frac{\Gamma(\nu_{\text{obs}})}{42 \text{ Gpc}^3} \right) \left( \frac{\nu_{\text{obs}}}{700 \text{ THz}} \right)^{-3} \left( \frac{\Omega_{\text{pixel}}}{3'' \times 3''} \right)^{-1} \left( \frac{\mathcal{R}}{800} \right)$$

$$\frac{P_{\text{COMAP}}^{\epsilon_I}}{70 \text{ Mpc}^3 (\text{kJy/sr})^2} \approx \left( \frac{T_{\text{system}}}{40 \text{ K}} \right)^2 \left( \frac{\tau_{\text{survey}}}{5000 \text{ hr}} \right)^{-1} \left( \frac{\Gamma(\nu_{\text{obs}})}{42 \text{ Gpc}^3} \right) \left( \frac{\nu_{\text{obs}}}{30 \text{ GHz}} \right)^2 \left( \frac{\Omega_{\text{field}}}{12 \text{ deg}^2} \right) \left( \frac{N_{\text{feeds}}}{19} \right)^{-1}$$

$$\frac{P_{\text{CCAT}}^{\epsilon_I}}{2.22 \times 10^4 \text{ Mpc}^3 (\text{kJy/sr})^2} \approx \left( \frac{P_{\delta V}^{\epsilon_F}(z=3.5)}{(5.7 \times 10^4 \text{ Jy/sr})^2} \right) \left( \frac{\Omega_{\text{pixel}}}{\frac{30'' \times 30''}{8 \ln 2}} \right) \left( \frac{\Gamma(z=3.5)}{40 \text{ Gpc}^3} \right) \left( \frac{\delta_\nu}{4.2 \text{ MHz}} \right)$$

$$\frac{P_{\text{SPHEREx}}^{\epsilon_I}}{4.1 \text{ Mpc}^3 (\text{kJy/sr})^2} \text{ Cov} \gtrsim [(LIM)^2 + (LIM \text{ Noise})^2] \left( \frac{\Omega_{\text{pixel}}}{6'' \times 6''} \right)^{-1} \left( \frac{N_{\text{eff}}}{2} \right)^{-1}$$



$$\left( \frac{T_{\text{system}}}{55 \text{ K}} \right)^2 \left( \frac{N_{\text{ant}}}{256} \right)^{-2} \left( \frac{N_{\text{pol}}}{2} \right)^{-1} \left( \frac{N_{\text{cyl}}}{4} \right)^{-2} \\ \left( \frac{\Delta b^2}{10^4 \text{ m}^2} \right)^2 \left( \frac{d_{\text{ant}}}{0.3048 \text{ m}} \right)^{-3} \left( \frac{w_{\text{cyl}}}{20 \text{ m}} \right)^{-2} \left( \frac{\eta}{0.7} \right)^{-3}$$

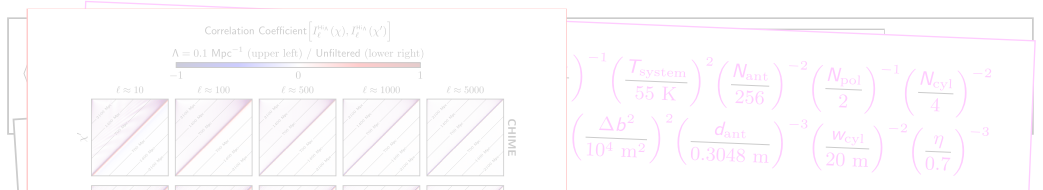
$$\left( \frac{\Gamma(\nu_{\text{obs}})}{42 \text{ Gpc}^3} \right) \left( \frac{\nu_{\text{obs}}}{700 \text{ THz}} \right)^{-3} \left( \frac{\Omega_{\text{pixel}}}{3'' \times 3''} \right)^{-1} \left( \frac{\mathcal{R}}{800} \right)$$

$$\left( \frac{\Gamma(\nu_{\text{obs}})}{42 \text{ Gpc}^3} \right) \left( \frac{\nu_{\text{obs}}}{30 \text{ GHz}} \right)^2 \left( \frac{\Omega_{\text{field}}}{12 \text{ deg}^2} \right) \left( \frac{N_{\text{feeds}}}{19} \right)^{-1}$$

$$\left( \frac{3.5}{\text{y/sr}^2} \right) \left( \frac{\Omega_{\text{pixel}}}{30'' \times 30''} \right) \left( \frac{\Gamma(z=3.5)}{40 \text{ Gpc}^3} \right) \left( \frac{\delta_{\nu}}{4.2 \text{ MHz}} \right)$$

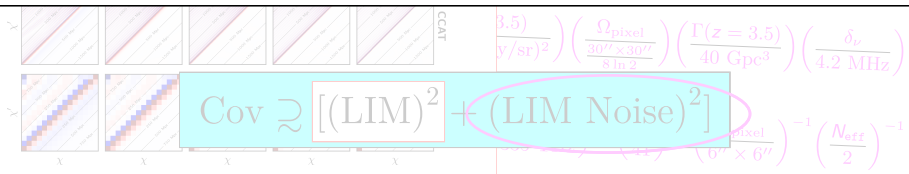
$$\left( \frac{\Omega_{\text{pixel}}}{6'' \times 6''} \right)^{-1} \left( \frac{N_{\text{eff}}}{2} \right)^{-1}$$

$$\text{Cov} \gtrsim [(LIM)^2 + (LIM \text{ Noise})^2]$$



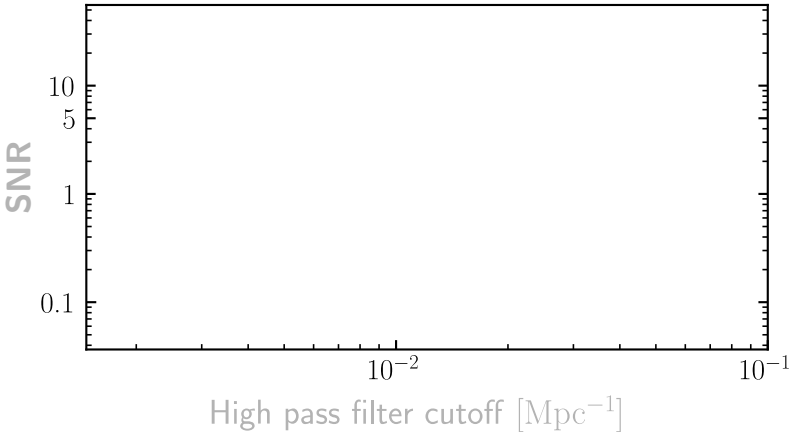
$$\left( \frac{T_{\text{system}}}{55 \text{ K}} \right)^2 \left( \frac{N_{\text{ant}}}{256} \right)^{-2} \left( \frac{N_{\text{pol}}}{2} \right)^{-1} \left( \frac{N_{\text{cyl}}}{4} \right)^{-2} \\ \left( \frac{\Delta b^2}{10^4 \text{ m}^2} \right)^2 \left( \frac{d_{\text{ant}}}{0.3048 \text{ m}} \right)^{-3} \left( \frac{w_{\text{cyl}}}{20 \text{ m}} \right)^{-2} \left( \frac{\eta}{0.7} \right)^{-3}$$

$$\mathbf{SNR}^2 \sim \langle \text{LIM}_{\ell}(\chi) \kappa_{-\ell} \rangle \cdot [\text{Cov}(\chi, \chi')]^{-1} \cdot \langle \text{LIM}_{\ell}(\chi') \kappa_{-\ell} \rangle$$



# Detectability of LIM $\times$ SO

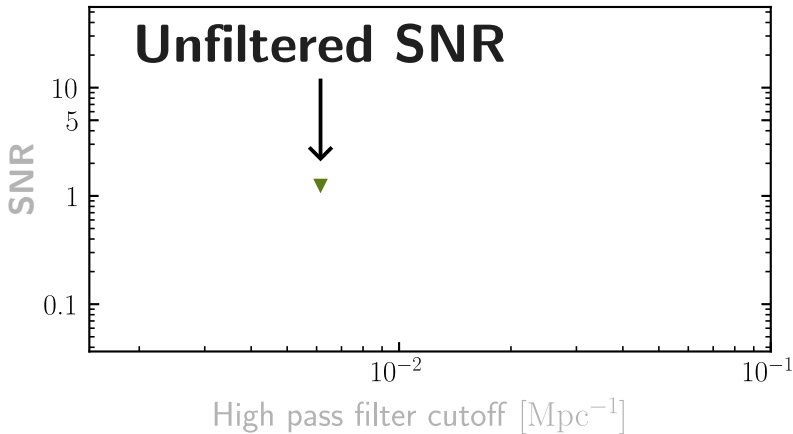
How detectable  
is direct correlation...



...as you filter out more modes

# Detectability of LIM $\times$ SO

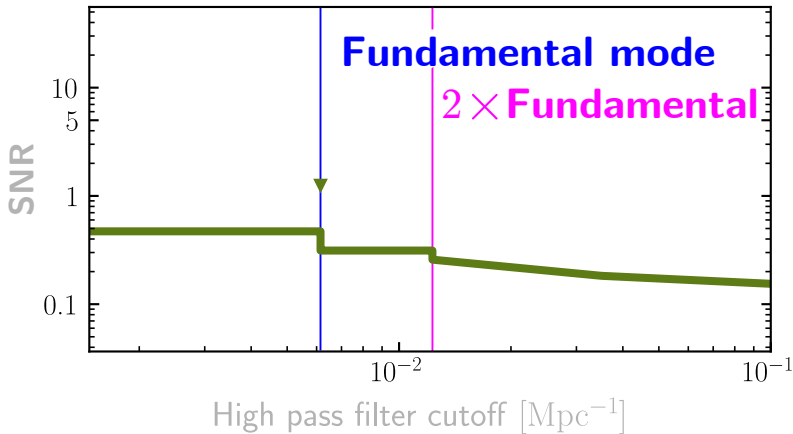
How detectable  
is direct correlation...



...as you filter out more modes

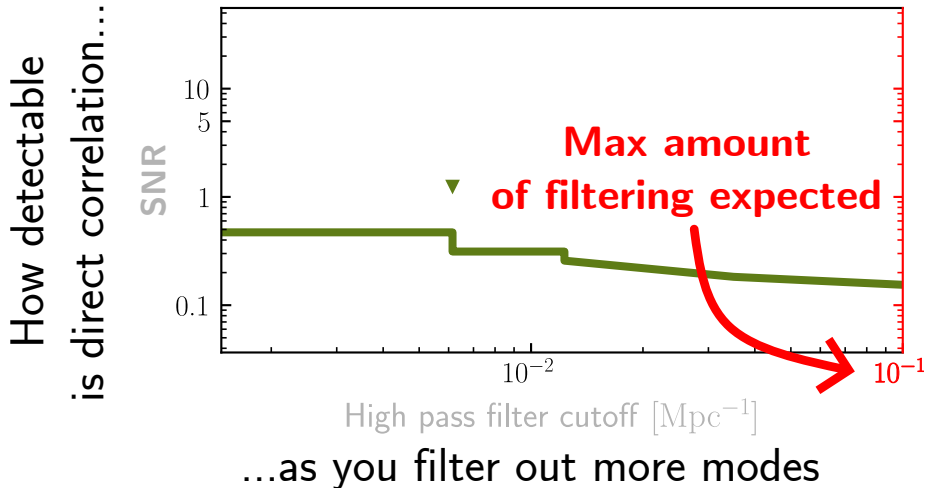
# Detectability of LIM $\times$ SO

How detectable  
is direct correlation...

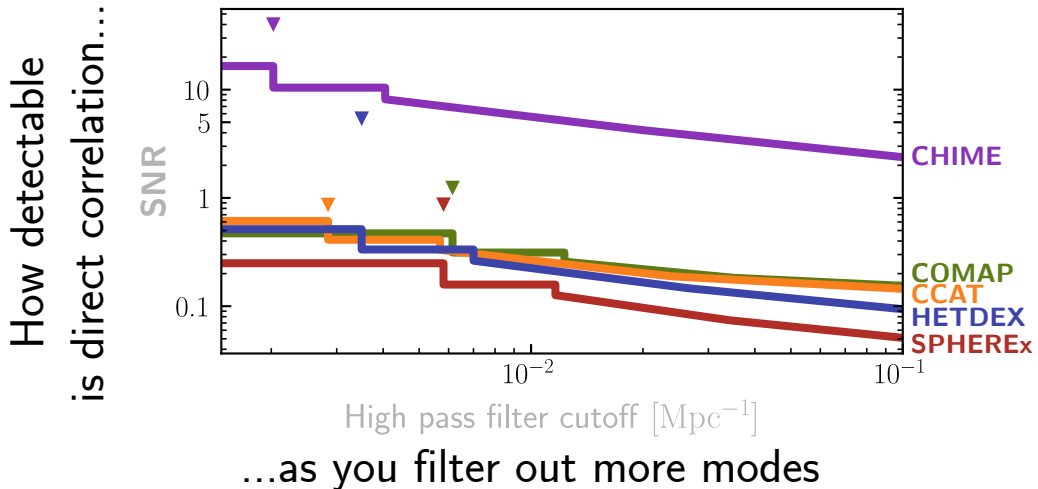


...as you filter out more modes

# Detectability of LIM $\times$ SO



# Detectability of LIM $\times$ SO

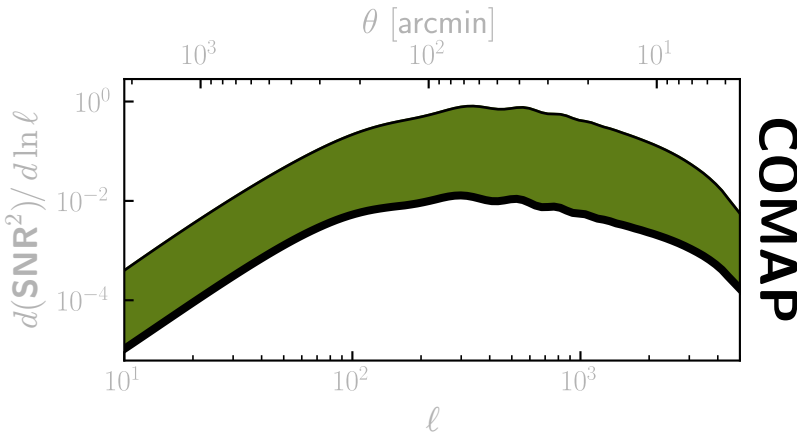


How detectable  
is direct correlation...



# Detectability of LIM $\times$ SO

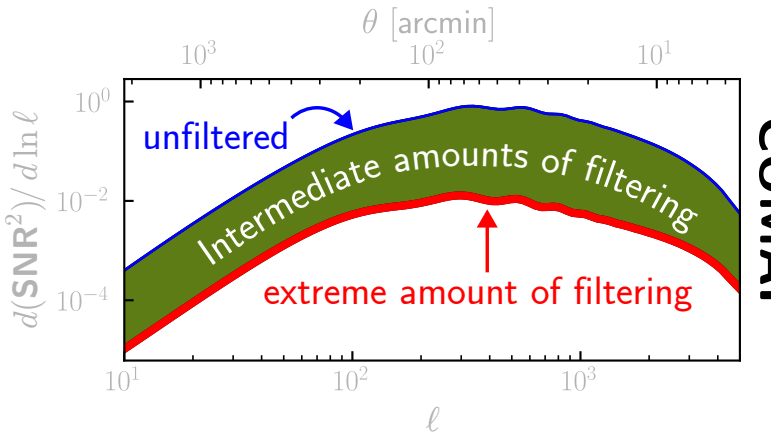
How detectable  
is direct correlation...



...on these angular scales

COMAP

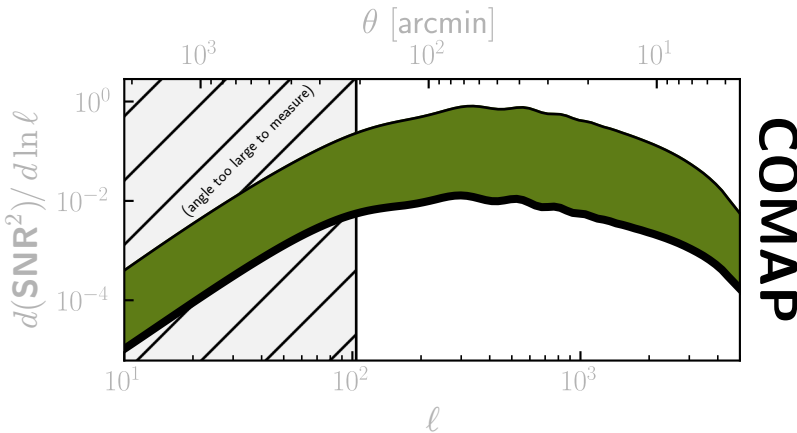
How detectable  
is direct correlation...



...on these angular scales

CO-MAP

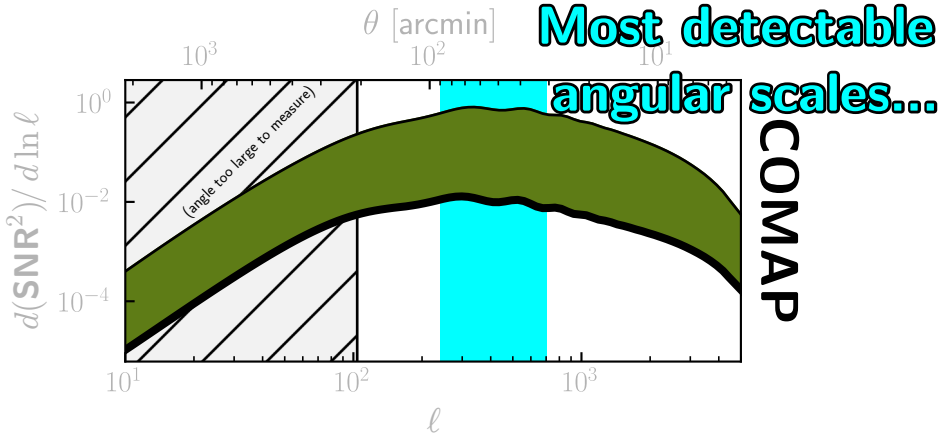
How detectable  
is direct correlation...



...on these angular scales

# Angular distribution of SNR

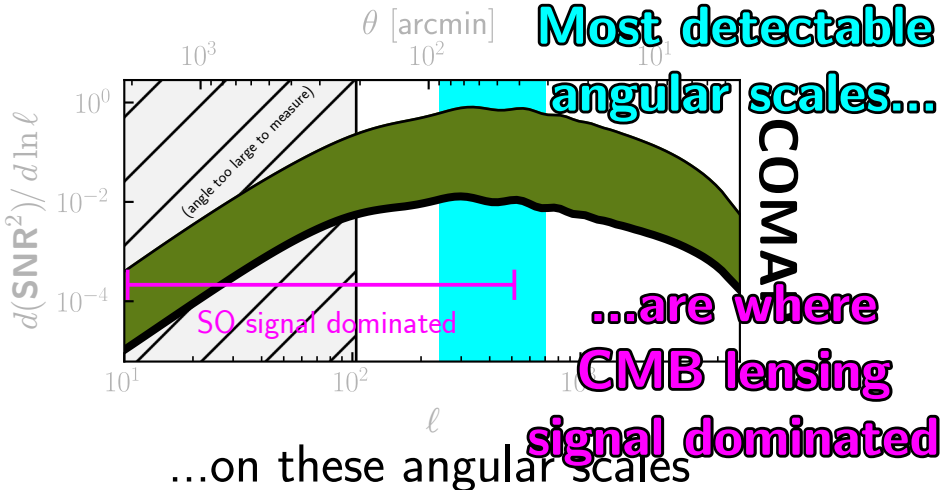
How detectable  
is direct correlation...



...on these angular scales

COMP

How detectable  
is direct correlation...



# Angular distribution of SNe

How detectable  
is direct observation?

Perfect CMB experiment  
→ roughly 3 times more  
detectable

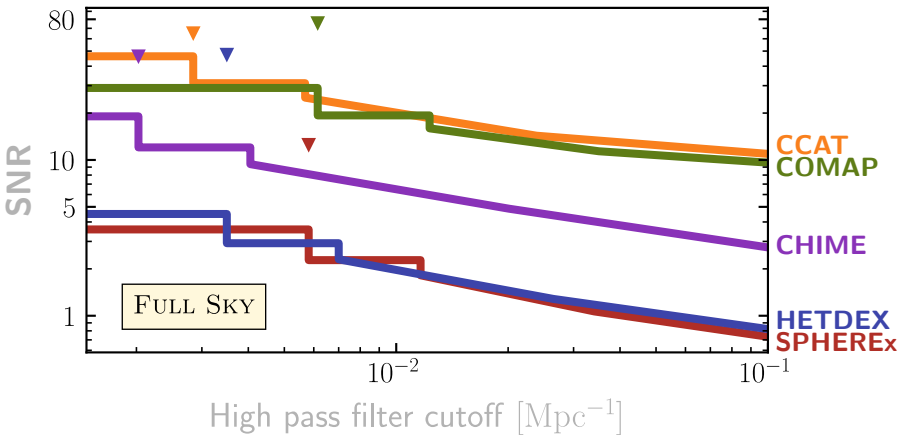
CMB lensing

...on these angular scales

signal dominated

How detectable  
is direct correlation...

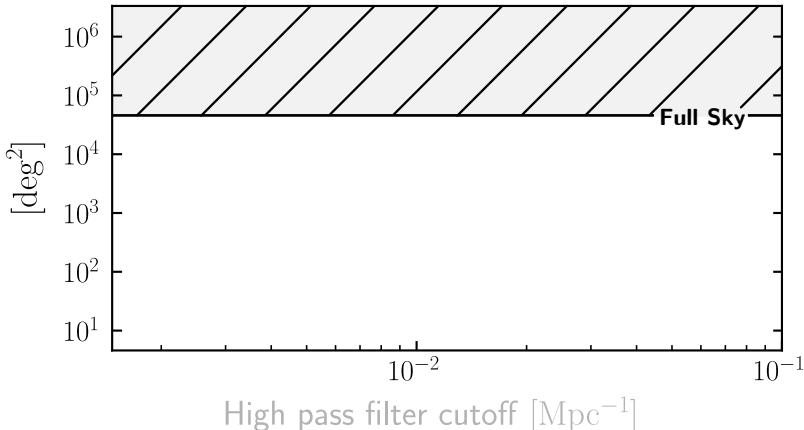
# Detectability of LIM $\times$ SO if we measured the **full sky**



...as you filter out more modes

How much sky area needed  
to detect direct correlation...

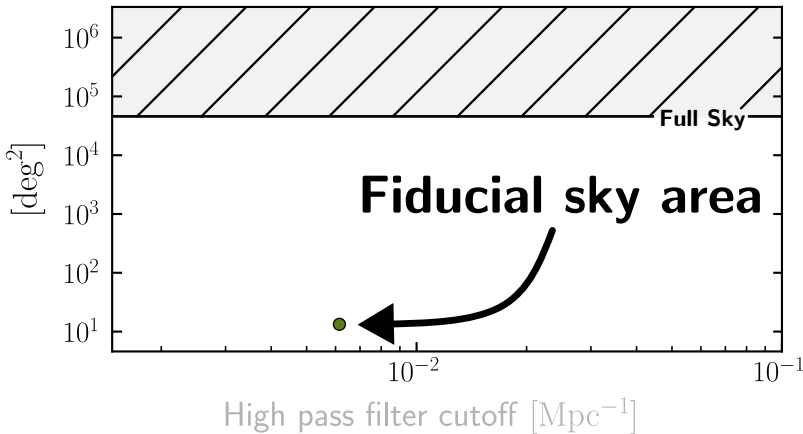
## Sky area to detect LIM $\times$ SO



...as you filter out more modes

How much sky area needed  
to detect direct correlation...

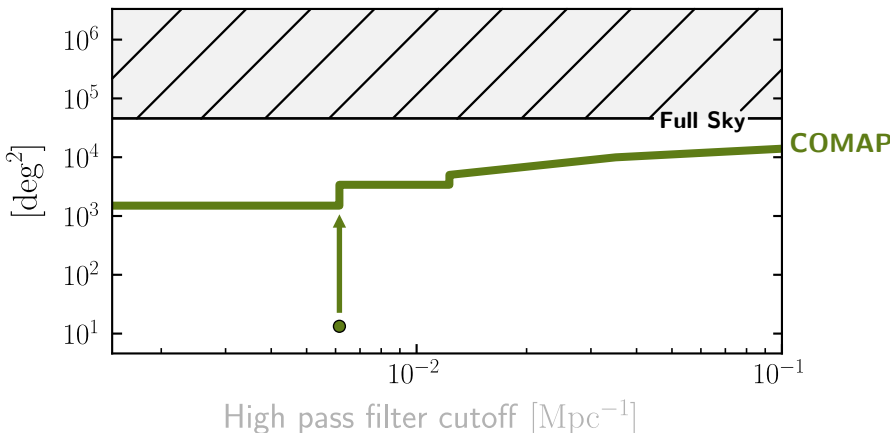
## Sky area to detect LIM $\times$ SO



...as you filter out more modes

How much sky area needed  
to detect direct correlation...

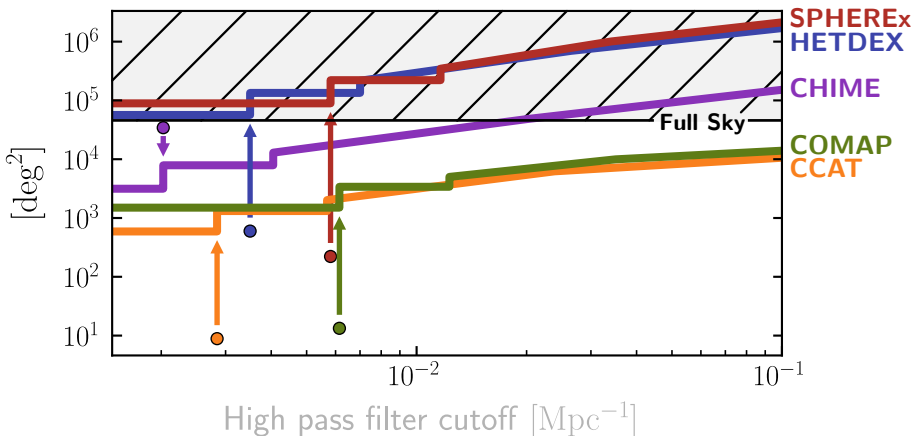
## Sky area to detect LIM $\times$ SO



...as you filter out more modes

How much sky area needed  
to detect direct correlation...

# Sky area to detect LIM $\times$ SO



...as you filter out more modes

# Conclusion

Evolution along the lightcone enables LIM to be directly correlated with CMB lensing despite bright foregrounds. More generally, bright foregrounds do not kill

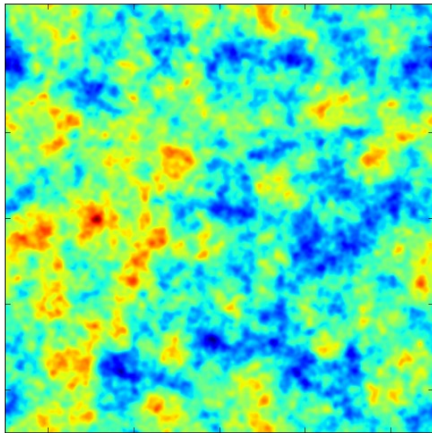
$\langle \text{LIM} \times [\text{your favorite projected field}] \rangle$ ,

reviving a lot of LIM science previously assumed hopeless.

Extra

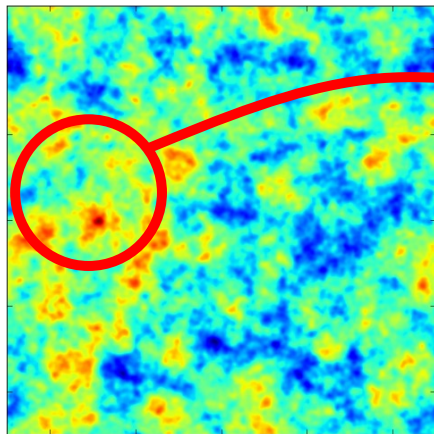
We can estimate lensing potential since  
**lensing breaks symmetry of CMB**

We can estimate lensing potential since  
**lensing breaks symmetry of CMB**

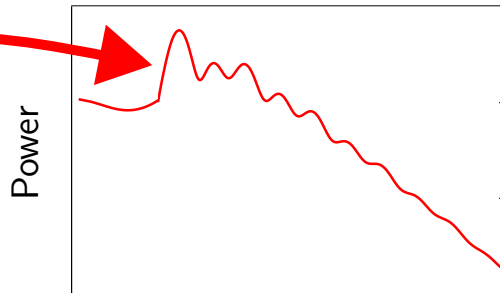


Unlensed CMB: **Statistically Homogeneous**

We can estimate lensing potential since  
**lensing breaks symmetry of CMB**

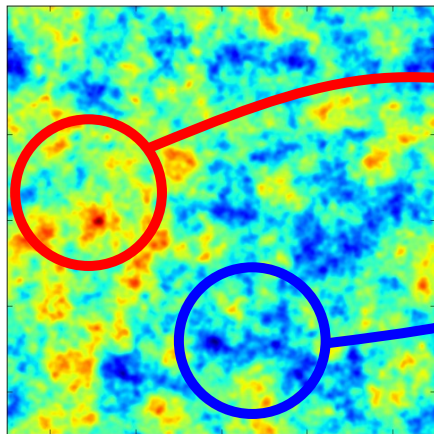


Unlensed CMB: **Statistically Homogeneous**

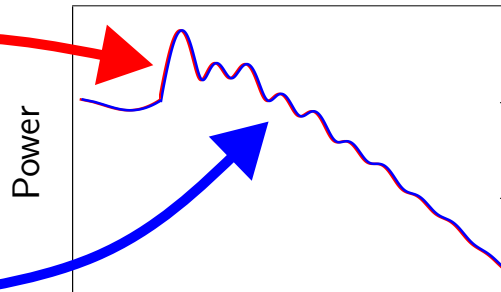


Angular Scale

We can estimate lensing potential since  
**lensing breaks symmetry of CMB**

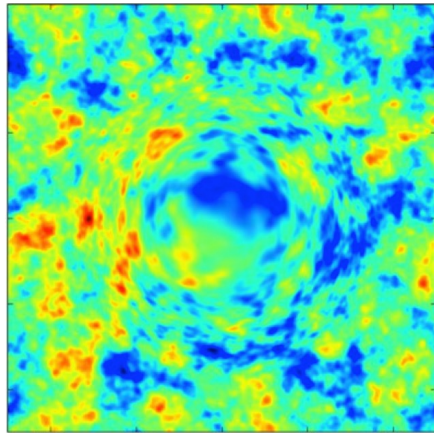


Unlensed CMB: **Statistically Homogeneous**



Lensed CMB: Power Spectrum Anisotropic

We can estimate lensing potential since  
**lensing breaks symmetry of CMB**



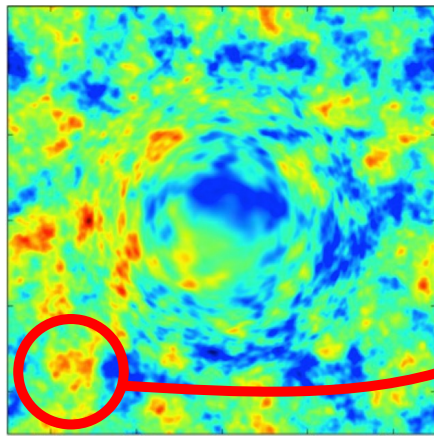
Power

Lensed CMB: ~~Statistically Homogeneous~~

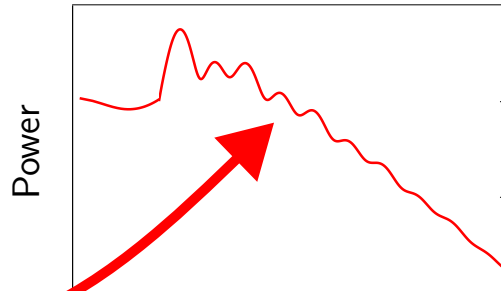


Angular Scale

We can estimate lensing potential since  
**lensing breaks symmetry of CMB**

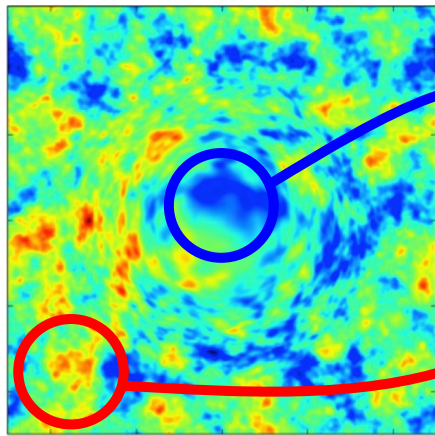


Lensed CMB: ~~Statistically Homogeneous~~

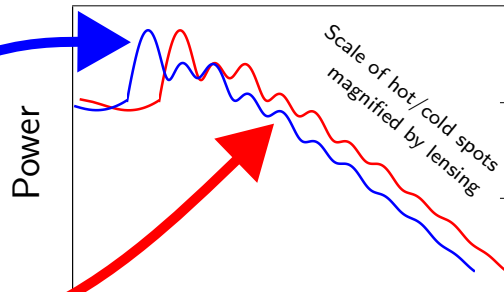


Angular Scale

We can estimate lensing potential since  
**lensing breaks symmetry of CMB**



Lensed CMB: ~~Statistically Homogeneous~~



Angular Scale

For a statistically **homogeneous** field like the unlensed CMB different Fourier modes are statistically independent:

$$\langle T_{\ell}^{\text{unlensed}} T_{L-\ell}^{\text{unlensed}} \rangle = 0$$

For a statistically **homogeneous** field like the unlensed CMB different Fourier modes are statistically independent:

$$\langle T_\ell^{\text{unlensed}} T_{\mathbf{L}-\ell}^{\text{unlensed}} \rangle = 0$$

Lensing of the CMB breaks this symmetry by inducing correlations in our lensed CMB:

$$\langle T_\ell T_{\mathbf{L}-\ell} \rangle \sim \kappa_{\mathbf{L}}$$

$$(\kappa \equiv -\nabla^2(\text{Lensing Potential})/2)$$

For a statistically **homogeneous** field like the unlensed CMB different Fourier modes are statistically independent:

$$\langle T_\ell^{\text{unlensed}} T_{\mathbf{L}-\ell}^{\text{unlensed}} \rangle = 0$$

Lensing of the CMB breaks this symmetry by inducing correlations in our lensed CMB:

$$\langle T_\ell T_{\mathbf{L}-\ell} \rangle \sim \kappa_{\mathbf{L}}$$

$$(\kappa \equiv -\nabla^2(\text{Lensing Potential})/2)$$

So correlations that we do see in our map give us information about the lensing allowing us to build an **quadratic estimator** (QE) of  $\kappa$  out of these correlations.

$$\hat{\kappa}_{\mathbf{L}} \sim \int_\ell T_\ell T_{\mathbf{L}-\ell}$$

CO rotational transition modeling follows COMAP21

$$\frac{L_{\text{CO}(1 \rightarrow 0)}(M_h)}{L_\odot} = 4.9 \times 10^{-5} \times \frac{C}{(M_h/M)^A + (M_h/M)^B}. \quad (1)$$

$A = -2.85$ ,  $B = -0.42$ ,  $\log C = 10.63$ , and  $\log M/M_\odot = 12.3$ .

[CII] emission modeling informed by Zhou+23

$$\log \frac{L_{[\text{CII}]}(M_h, z)}{L_\odot} = \alpha \log \frac{\text{SFR}(M_h, z)}{M_\odot/\text{yr}} + \beta. \quad (2)$$

$\alpha = 1.26$  and  $\beta = 7.1$ .

## Ly- $\alpha$ luminosity modeling informed by Chung+18

$$\frac{L_{\text{Ly-}\alpha}(M_h, z)}{\text{erg/s}} = 1.6 \times 10^{42} \left( \frac{\text{SFR}(M_h, z)}{M_\odot/\text{yr}} \right) f_{\text{esc}}(\text{SFR}, z). \quad (3)$$

1.  $f_{\text{esc}}$  increases monotonically with redshift; and
2.  $f_{\text{esc}}$  decreases with higher SFR.

This motivates the parameterization of  $f_{\text{esc}}$ :

$$f_{\text{esc}}(\text{SFR}, z) = \left[ \frac{\left( f_0 + \frac{1-f_0}{1+(\text{SFR}/\text{SFR}_0)^\eta} \right)}{(1 + e^{-\xi(z-z_0)})^\zeta} \right]^2.$$

$\xi = 1.6$ ,  $\zeta = 1/4$ ,  $\eta = 0.875$ ,  $z_0 = 3.125$ ,  $f_0 = 0.18$ , and  $\text{SFR}_0 = 1.29 M_\odot/\text{yr}$ .

HI 21-cm luminosity modeling. Relate halo mass to neutral hydrogen mass  $M_{\text{HI}}$  with results derived from the TNG100 magneto-hydrodynamic simulation (Villaescusa-Navarro+18) and then relate neutral hydrogen mass to luminosity by considering only spontaneous emission:

$$L_{\text{HI}}(M, z) = A_{10} \times h\nu_{21} \times \frac{3}{4} \frac{M_{\text{HI}}(M, z)}{m_p}. \quad (4)$$

$A_{10} \simeq 2.869 \times 10^{-15} \text{ s}^{-1}$  is the Einstein spontaneous emission coefficient for the 21-cm hyperfine line of HI,  $m_p$  is the mass of the proton, and  $M_{\text{HI}}(M, z)$  is modeled with the parameterization of (Villaescusa-Navarro+18)

$$M_{\text{HI}}(M_h, z) = \frac{M_0(z) (M_h/M_{\min}(z))^{\alpha(z)}}{\exp \left\{ (M_{\min}(z)/M_h)^{0.35} \right\}}. \quad (5)$$

Informed by TNG100 we determine  $M_0(z)$ ,  $M_{\min}(z)$  and  $\alpha(z)$  by linearly interpolating the best-fit values of these quantities reported at redshift  $z = 0, 1, 2, 3, 4, 5$  in Table 1 of (Villaescusa-Navarro+18).

$$\frac{P_{\text{CHIME}}^{\epsilon_I}}{0.83 \text{ Mpc}^3 \text{ (kJy/sr)}^2} \approx \left( \frac{\Omega_{\text{field}}}{31000 \text{ deg}^2} \right) \left( \frac{\tau_{\text{survey}}}{1 \text{ yr}} \right)^{-1} \left( \frac{T_{\text{system}}}{55 \text{ K}} \right)^2 \left( \frac{N_{\text{ant}}}{256} \right)^{-2} \left( \frac{N_{\text{pol}}}{2} \right)^{-1} \left( \frac{N_{\text{cyl}}}{4} \right)^{-2} \\ \left( \frac{\nu_{\text{obs}}}{663 \text{ MHz}} \right) \left( \frac{\Gamma(\nu_{\text{obs}})}{32.1 \text{ Gpc}^3} \right) \left( \frac{\Delta b^2}{10^4 \text{ m}^2} \right)^2 \left( \frac{d_{\text{ant}}}{0.3048 \text{ m}} \right)^{-3} \left( \frac{w_{\text{cyl}}}{20 \text{ m}} \right)^{-2} \left( \frac{\eta}{0.7} \right)^{-3}$$

$$\frac{P_{\text{HETDEX}}^{\epsilon_I}}{1.14 \text{ Mpc}^3 \text{ (kJy/sr)}^2} \approx \left( \frac{P_{\delta V}^{\epsilon_F}}{10^{-34} \text{ erg}^2 \text{ s}^{-2} \text{ cm}^{-4}} \right) \left( \frac{\Gamma(\nu_{\text{obs}})}{42 \text{ Gpc}^3} \right) \left( \frac{\nu_{\text{obs}}}{700 \text{ THz}} \right)^{-3} \left( \frac{\Omega_{\text{pixel}}}{3'' \times 3''} \right)^{-1} \left( \frac{\mathcal{R}}{800} \right)$$

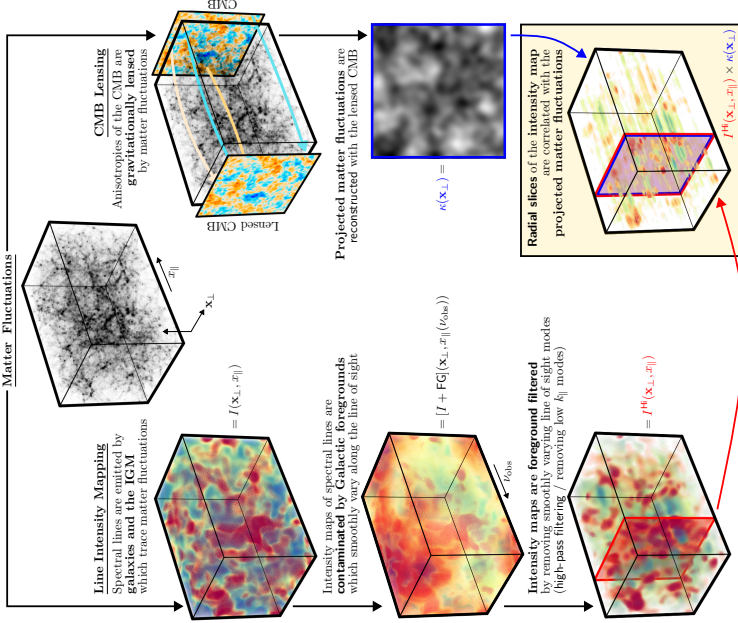
$$\frac{P_{\text{COMAP}}^{\epsilon_I}}{70 \text{ Mpc}^3 \text{ (kJy/sr)}^2} \approx \left( \frac{T_{\text{system}}}{40 \text{ K}} \right)^2 \left( \frac{\tau_{\text{survey}}}{5000 \text{ hr}} \right)^{-1} \left( \frac{\Gamma(\nu_{\text{obs}})}{42 \text{ Gpc}^3} \right) \left( \frac{\nu_{\text{obs}}}{30 \text{ GHz}} \right)^2 \left( \frac{\Omega_{\text{field}}}{12 \text{ deg}^2} \right) \left( \frac{N_{\text{feeds}}}{19} \right)^{-1}$$

$$\frac{P_{\text{CCAT}}^{\epsilon_I}}{2.22 \times 10^4 \text{ Mpc}^3 \text{ (kJy/sr)}^2} \approx \left( \frac{P_{\delta V}^{\epsilon_I}(z=3.5)}{(5.7 \times 10^4 \text{ Jy/sr})^2} \right) \left( \frac{\Omega_{\text{pixel}}}{\frac{30'' \times 30''}{8 \ln 2}} \right) \left( \frac{\Gamma(z=3.5)}{40 \text{ Gpc}^3} \right) \left( \frac{\delta_\nu}{4.2 \text{ MHz}} \right)$$

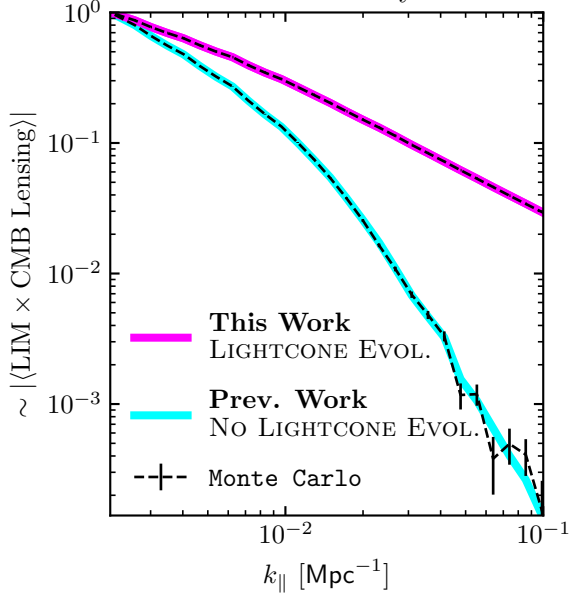
$$\frac{P_{\text{SPHEREx}}^{\epsilon_I}}{4.1 \text{ Mpc}^3 (\text{kJy/sr})^2} \approx \left( \frac{P_{\text{PS}}^{\epsilon_f}}{(1.15 \text{ } \mu\text{Jy})^2} \right) \left( \frac{\Gamma(\nu_{\text{obs}})}{29.2 \text{ Gpc}^3} \right) \left( \frac{\nu_{\text{obs}}}{335 \text{ THz}} \right)^{-1} \left( \frac{\mathcal{R}}{41} \right)^{-1} \left( \frac{\Omega_{\text{pixel}}}{6'' \times 6''} \right)^{-1} \left( \frac{N_{\text{eff}}}{2} \right)^{-1}$$

<b>Experiment</b>	<b>CHIME</b>	<b>HETDEX</b>	<b>COMAP</b>	<b>CCAT</b>	<b>SPHEREx</b>
Line	HI(21cm)	Ly- $\alpha$	CO(1→0)	[CII]	Ly- $\alpha$
$\nu_{\text{rest}}$	1420.406 MHz	2456.43 THz	115.27 GHz	1900.5 GHz	2456.43 THz
$\nu_{\text{obs}}$	617-710 MHz	545-857 THz	26-34 GHz	210-420 GHz	270-400 THz
$z_{\text{obs}}$	1.0 - 1.3	1.9 - 3.5	2.4 - 3.4	3.5 - 8.1	5.2 - 8
$\mathcal{R}$	1700	800	800	100	41
$\Omega_{\text{field}} \text{ [deg}^2\text{]}$	31000	540	12	8	200
$\sqrt{\Omega_{\text{pixel}}}$	40'	3''	$4.5'/\sqrt{8 \ln 2}$	$30''/\sqrt{8 \ln 2}$	6''

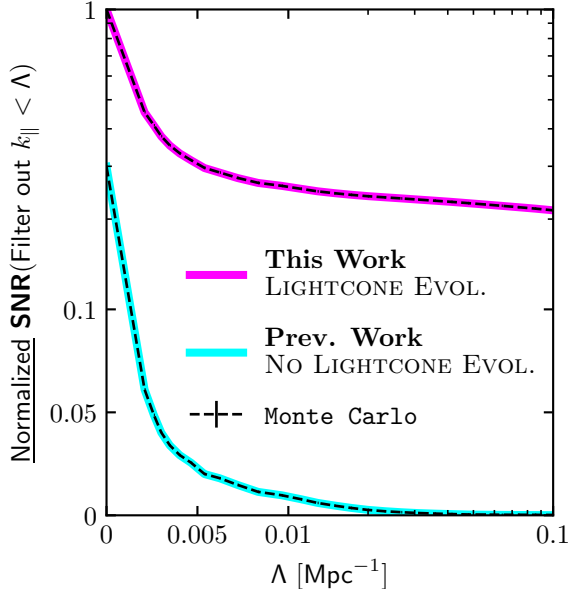
### Direct correlation of foreground filtered Line Intensity Maps with CMB Lensing



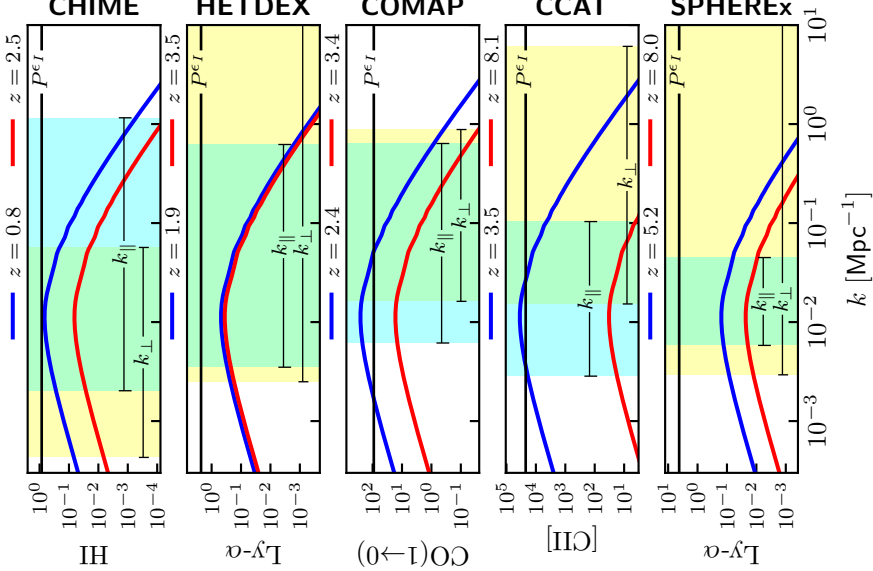
## Intuition from Toy Model



## Detectability in Toy Model

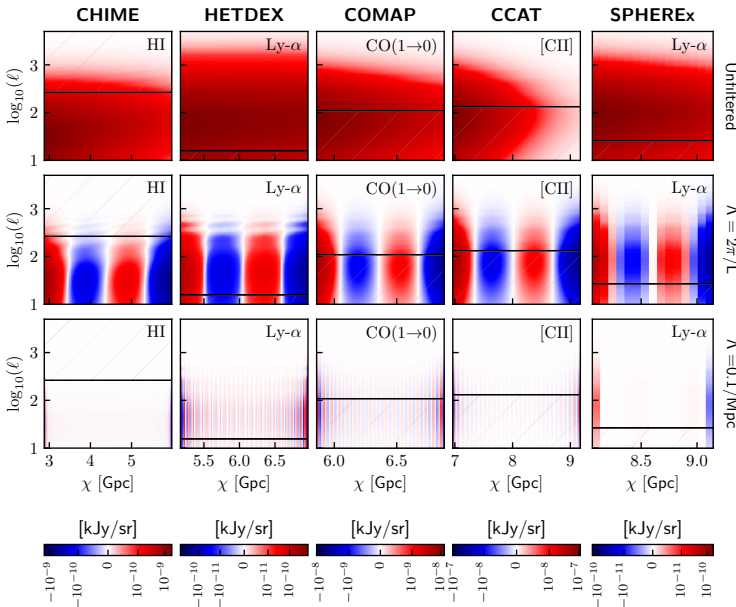


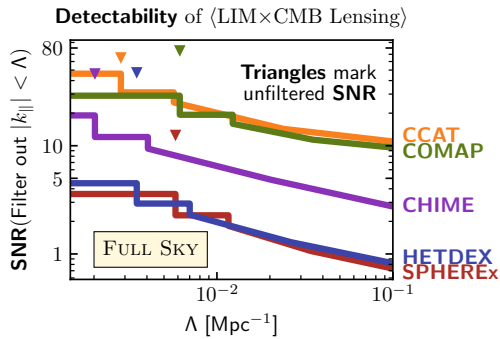
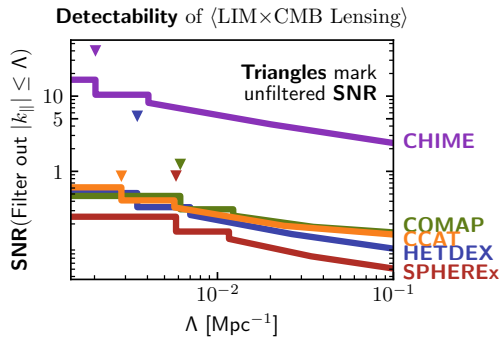
## Spectral Line Emission Models



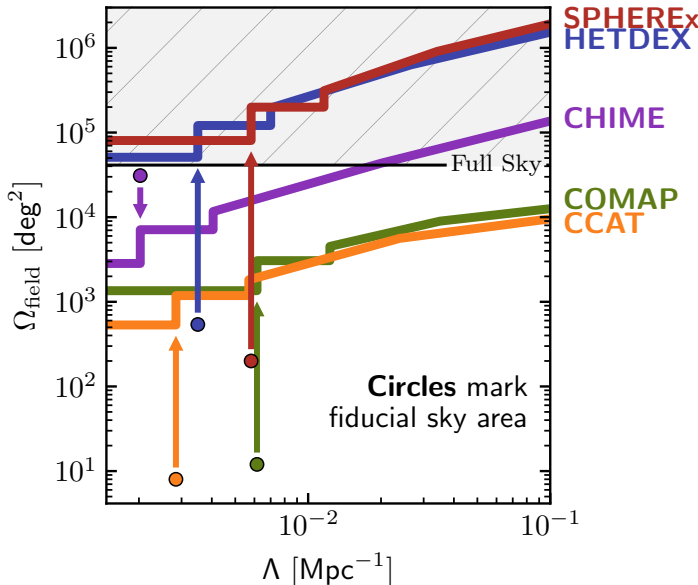
$$K_{\text{LIM}}^2(z) P_{\text{lim}}^m(k, z=0) [(\text{kJy/sr})^2 \text{Mpc}^3]$$

### **⟨Foreground Filtered LIM × CMB Lensing⟩**

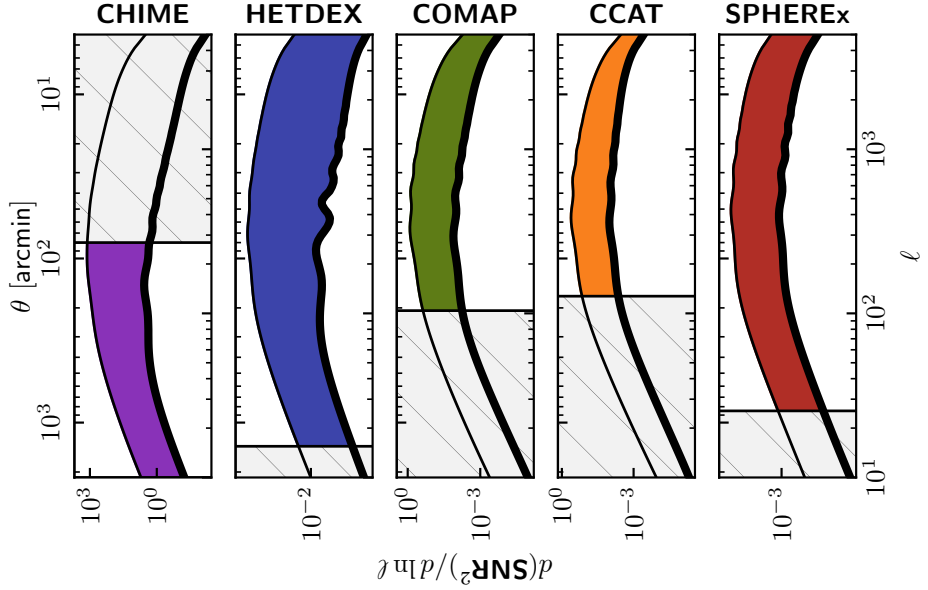




## Sky Area to detect $\langle \text{LIM} \times \text{CMB Lensing} \rangle$

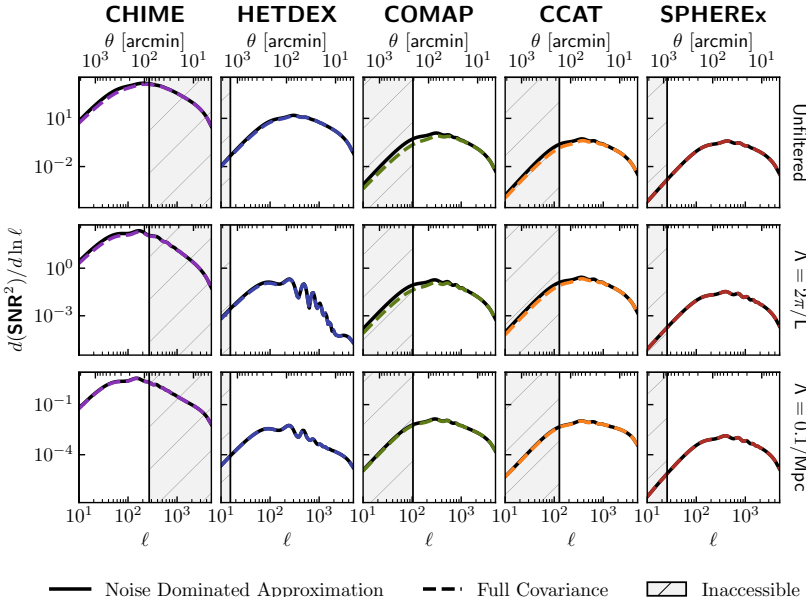


### Angular distribution of SNR

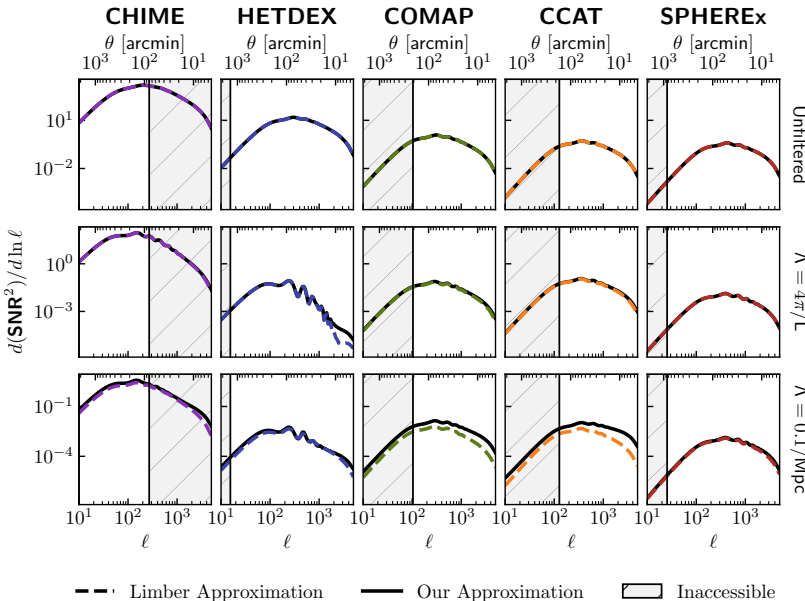


— Unfiltered —  $\Lambda = 0.1/\text{Mpc}$

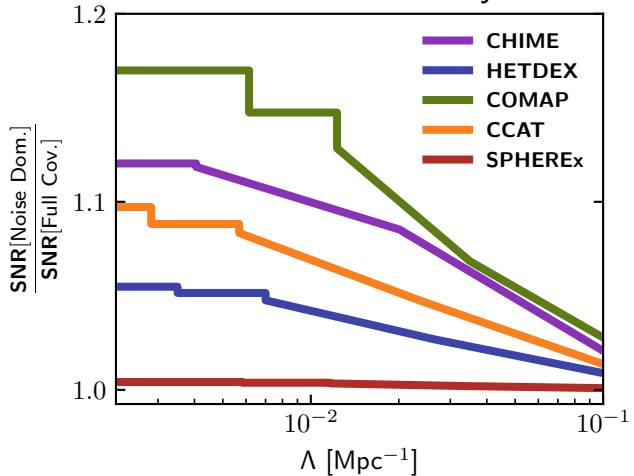
# Noise Dominated vs. Full Covariance Effect on Angular Distribution of SNR



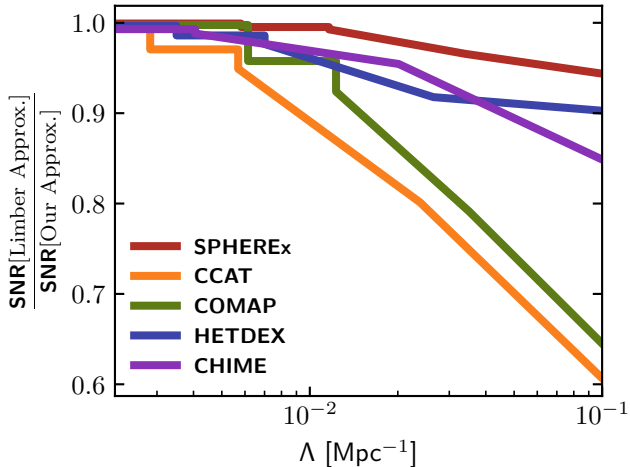
# Limber vs. Our Approximation Effect on Angular Distribution of SNR



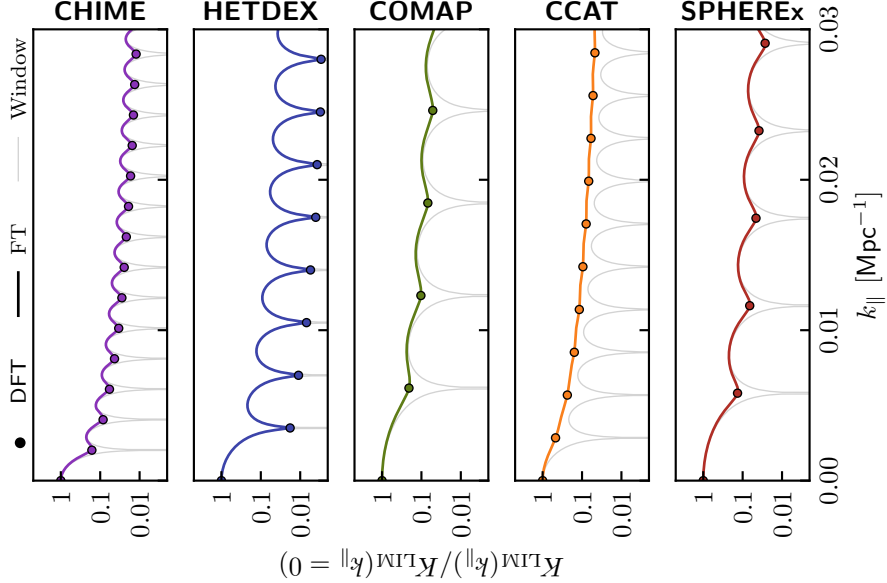
## Noise Dominated vs. Full Covariance Effect on Detectability



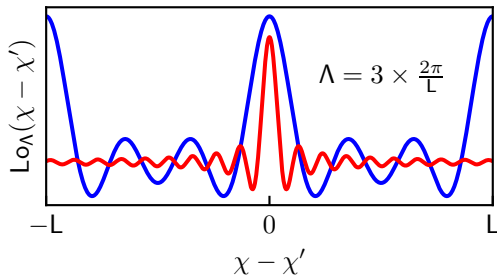
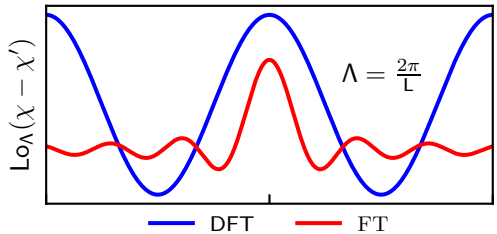
## Limber vs. Our Approximation Effect on Detectability



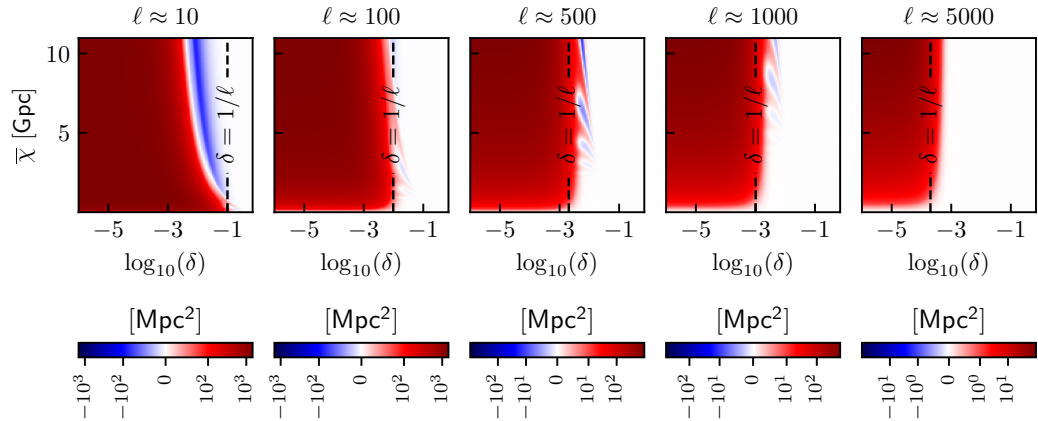
# FOURIER TRANSFORM of Evolution Kernels



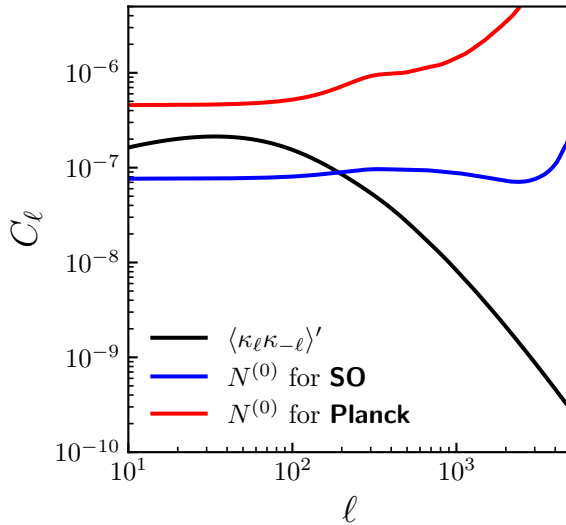
## Discrete vs. Continuous Filtering



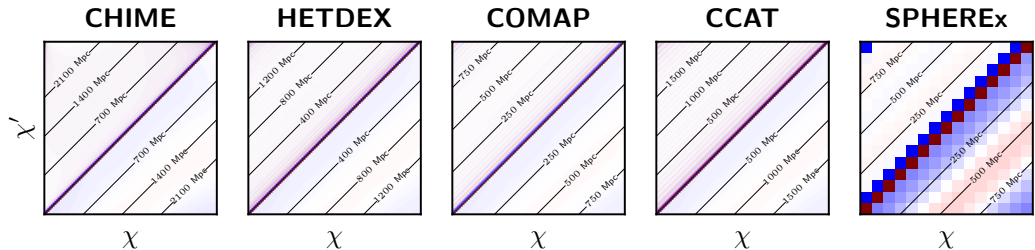
# ANGULAR SPECTRUM of Line-of-Sight CORRELATION FUNCTIONS $\xi_\ell(\bar{\chi}, \delta)$



## CMB Lensing Spectrum



## Correlation between LIM Instrumental Noise Redshift Bins

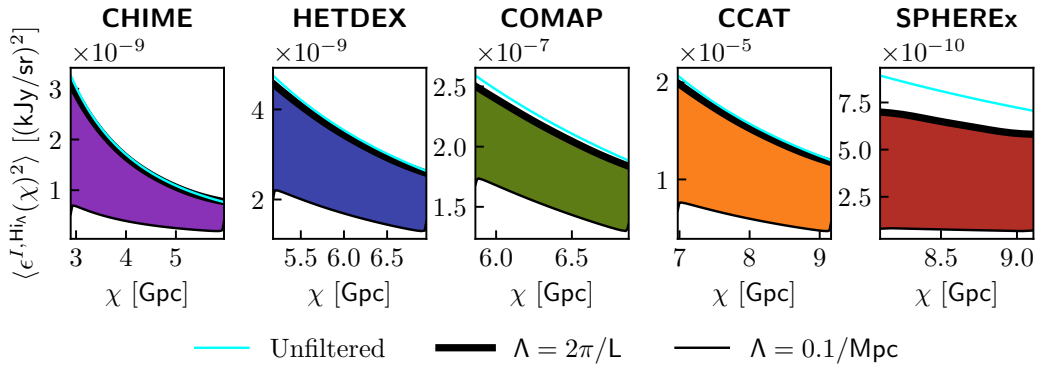


$$\Lambda = 0.1 \text{ Mpc}^{-1} \text{ (upper left)} / \Lambda = \frac{2\pi}{L} \text{ (lower right)}$$

A horizontal color bar with a gradient from blue to red. It has numerical labels -1, 0, and 1 below it, corresponding to the color scale.

Correlation Coefficient  $[\epsilon^{I,\text{Hi}\Lambda}(\chi), \epsilon^{I,\text{Hi}\Lambda}(\chi')]$

## Variance of LIM Instrumental Noise Redshift Bins



**Correlation between Line Intensity Map Redshift Bins**

